

Scaling Model Checking for DNN Analysis via State-Space Reduction and Input Segmentation (Extended Version)

MAHUM NASEER, Institute of Computer Engineering, Vienna University of Technology, Austria

OSMAN HASAN, School of Electrical Engineering & Computer Science (SEECs), National University of Sciences & Technology (NUST), Pakistan

MUHAMMAD SHAFIQUE, Division of Engineering, New York University Abu Dhabi (NYUAD), United Arab Emirates

Owing to their remarkable learning capabilities and performance in real-world applications, the use of machine learning systems based on Neural Networks (NNs) has been continuously increasing. However, various case studies and empirical findings in the literature suggest that slight variations to NN inputs can lead to erroneous and undesirable NN behavior. This has led to considerable interest in their formal analysis, aiming to provide guarantees regarding a given NN's behavior. Existing frameworks provide robustness and/or safety guarantees for the trained NNs, using satisfiability solving and linear programming. We proposed FANNet, the first model checking-based framework for analyzing a broader range of NN properties. However, the state-space explosion associated with model checking entails a scalability problem, making the FANNet applicable only to small NNs. This work develops state-space reduction and input segmentation approaches, to improve the scalability and timing efficiency of formal NN analysis. Compared to the state-of-the-art FANNet, this enables our new model checking-based framework to reduce the verification's timing overhead by a factor of up to 8000, making the framework applicable to NNs even with approximately 80 times more network parameters. This in turn allows the analysis of NN safety properties using the new framework, in addition to all the NN properties already included with FANNet. The framework is shown to be efficiently able to analyze properties of NNs trained on healthcare datasets as well as the well-acknowledged ACAS Xu NNs.

CCS Concepts: • **Theory of computation** → **Verification by model checking**; Divide and conquer; • **Computing methodologies** → *Neural networks*.

Additional Key Words and Phrases: Bias, Formal Analysis, Input Node Sensitivity, Noise Tolerance, Robustness, State-Space Reduction

1 INTRODUCTION

The continuous improvement of Machine Learning (ML) systems, often wielding Neural Networks (NNs), has led to an ever-growing popularity of these systems in real-world applications. Owing to their efficient learning and re-learning capabilities, high classification accuracy for testing datasets, and adaptability via transfer learning, they often find their way to numerous classification and decision-making tasks. These include face identification [73], speech recognition [30], anomaly detection [57], and even safety critical applications like autonomous driving [25] and healthcare [5, 24].

However, as observed in numerous recent works, the NNs deployed in such systems are rarely *resilient*, i.e., they are extremely susceptible to misclassify or arrive at an unsafe output decision in the presence of slight input modifications [50, 62]. These modifications can be in the form of imperceptible noise [36, 37], adversarial cues [27], backdoors [42], or simply affine and photometric transformations [50]. Earlier attempts to ensure correct functioning of these NNs

Authors' addresses: Mahum Naseer, Institute of Computer Engineering, Vienna University of Technology, Vienna, 1040, Austria, mahum.naseer@tuwien.ac.at; Osman Hasan, School of Electrical Engineering & Computer Science (SEECs), National University of Sciences & Technology (NUST), Islamabad, Pakistan, osman.hasan@seecs.nust.edu.pk; Muhammad Shafique, Division of Engineering, New York University Abu Dhabi (NYUAD), Abu Dhabi, United Arab Emirates, muhammad.shafique@nyu.edu.

involved empirical approaches, for instance using gradient based methods [46, 62] to identify the adversarial noise patterns that would lead the NN to misclassify benign inputs. Although such attempts provide evidence to the lack of resilience of NNs, they are insufficient to provide any guarantees regarding NNs’ resilience in the case when no adversarial noise is found.

To deal with the aforementioned problem, there has been a great interest towards the rigorous evaluation of NNs, using formal verification, in recent years [9, 35, 63]. This usually involves checking resilience properties, like robustness and safety, of the NNs using Satisfiability (SAT) checking or Linear Programming (LP). However, the exploration of formal approaches beyond SAT and LP, to analyze wider variety of NN’s properties, remains largely neglected.

To the best of our knowledge, our prior work on Formal Analysis of Neural Networks (FANNNet) [48] was the first attempt to analyze NN using model checking. The framework was applicable for the verification and analysis of multiple NN properties namely: robustness under constrained noise bounds, noise tolerance, training bias and input node sensitivity. *However, the FANNNet framework provided limited scalability for formal analysis owing to the large state–transition system it generated, even for relatively small NNs. Hence, the applicability of the framework was limited to small NNs only.*

This work introduces FANNNet+ ¹, an enhanced model checking–based formal analysis framework for NNs that overcomes the limitations of FANNNet, and provides significant improvement over FANNNet in terms of scalability, timing–efficiency and the scope of NN properties analyzed by the framework. In particular, **the novel contributions of this work are as follows:**

- (1) Providing novel state–space reduction techniques to reduce the size of the NN’s state–transition system (Section 5.1).
- (2) Providing coarse–grain and random input segmentation approaches, to split the input domain into more manageable sub–domains, to aid model checking (Section 5.2).
- (3) Leveraging the framework for the automated collection of a large database of counterexamples, which assist in an improved analysis of the sensitivity of input nodes and the detection of training bias (Section 5.3).
- (4) Comparing the timing overhead of simulation–based testing, FANNNet [48] and the proposed framework. The proposed framework reduces the timing–cost of model checking by a factor of up to 8000 (Section 7.1).
- (5) Making use of the input sub–domains to verify safety properties of NNs, in addition to robustness under constrained noise, noise tolerance, training bias and input node sensitivity properties (Section 7.4).
- (6) Deploying the above techniques to demonstrate the applicability of the new framework on NN case studies with up to 80 times more parameters than the ones used in FANNNet, thereby illustrating better scalability and applicability to more complex networks (Sections 6 and 7).

Paper Organization. The rest of the paper is organized as follows. Section 2 provides an overview of the formal analysis approaches available in the literature for NNs. Section 3 defines the basic NN and model checking concepts and formalism relevant to this paper. Section 4 gives a summary of the framework FANNNet. Section 5 provides an overview for our proposed framework FANNNet+ for the formal NN analysis, while elaborating on the proposed optimizations to improve the scalability, timing–efficiency and scope of addressed NN properties of the framework. Section 6 highlights the NNs and datasets used to demonstrate the applicability of our framework for the various NN properties. Section 7 presents the results of analysis for the given NNs, also comparing timing–overhead of testing, FANNNet and FANNNet+. Finally, Section 8 concludes the paper.

¹<https://github.com/Mahum123/FANNNetPlus>

2 RELATED WORK

The earliest attempt [72] to analyze correct NN behavior involved mapping an NN to a look-up table. However, the approach lacked the sophistication to allow the analysis of intricate NN properties. Recent works instead focus mainly on the use SAT solving and LP, which not only allow a better formal representation of NNs but also the analysis of NN properties like robustness and safety.

2.1 Satisfiability solving-based approaches

The SAT-based NN verification works by first translating NN and its properties in Conjunctive Normal Form (CNF), and then using automated SAT solvers to search for the satisfying inputs that lead to erroneous NN behavior [18, 58]. However, the complexity of the problem limits its widespread use in real-world NN: the theory of transcendental functions, sometimes used as the activation functions for NNs, is known to be undecidable [53], and the verification of NN even with piecewise linear activations is an NP-complete problem [34].

Earlier works [52, 54] focused on the safety properties of single hidden layer NNs with logistic function as the activation. More popular SAT-based approaches include the ones involving layer by layer NN analysis [32] and leveraging simplex algorithm to provide better splitting heuristics for piecewise linear activations during NN verification [34, 35]. Some of the recent works [14, 47, 55] focus on the verification of Binary Neural Networks (BNNs), which are shown to be more power-efficient for the real-world applications [33]. BNNs reduce the complexity of the verification task over conventional NNs by using binary valued parameters instead of the real numbered values.

In addition, the use of multiple abstraction techniques has also been proposed to reduce the complexity of SAT-based NN verification. These include input clustering [29], merging of the neurons in formal NN model [14, 23], and iterative approximation of a non-linear activation function to a piecewise linear activation function [51]. However, it must be noted that approaches involving the approximation of non-linear function into piecewise linear ones [51] may lead to *incompleteness* in verification results, i.e., the results may contain false positives.

2.2 Linear programming-based approaches

In contrast, the LP-based NN verification approaches translate the NN to a set of linear constraints. The property to be verified is in turn expressed as an objective function. This formulates an optimization problem [68] aimed at identifying the satisfying assignments to the linear constraints that lead to the minima/maxima of the objective, and hence constitute an input leading to an erroneous behavior of the NN.

Due to the inherent support of LP for the linear constraints, these approaches are often popular for the verification of NNs with piecewise linear (for instance, the ReLU) activations [6, 43, 66]. Branch and bound heuristics [9, 10, 66, 67] are also often deployed for an efficient implementation of LP. In addition, some works [8, 15, 20, 43, 63] also propose the use of Big-M technique, where an indicator variable is added to the linear constraints to distinguish the different linear regions of the piecewise linear activation function for NN verification.

The popular abstraction approaches to reduce the complexity of NN verification, pertinent to LP, include: over-approximation of the input domain [64, 65, 70, 71], approximation of the ReLU activation function [26, 59, 60], and merging of the neurons in NN layers [2]. In addition to these, experiment with the iterative deployment of both LP and SAT solvers over an overapproximated input domain was also proposed [21], to reduce the reachable output, and subsequently check network robustness and safety properties. Again, similar to the case for SAT-based approaches, such abstractions may render the verification *incomplete*.

3 PRELIMINARIES

This section describes the formalism of NN architecture and properties relevant to this paper. The basics of model checking, sufficient to understanding this work, are also provided. Interested readers may refer to [4] for more inclusive details on model checking.

3.1 Neural Network Architecture

Essentially, a NN is an interconnection of neurons arranged in input, output and hidden layers [61]. This work focuses on feed-forward fully-connected NNs, as shown in Fig. 1(a).

Definition 3.1 (Feed-forward fully-connected neural network). Given input domain X^0 , a feed-forward network $F : X^0 \rightarrow X^L$ maps the input to the output domain X^L such that the neurons in each layer k depends only on the inputs from the preceding layer $k - 1$. This results in a loop-free network that can be represented by $x^L = F(x^0) = f^L(f^{L-1}(\dots f^1(x^0)\dots))$, where f^k encapsulates the linear and non-linear transformations for layer k , $x^0 \in X^0$ is an input from the input domain, and $x^L \in X^L$ is an output class from the L classes in the output domain. The network is also fully-connected if each neuron in each network layer is connected to every neuron in the adjoining layer.

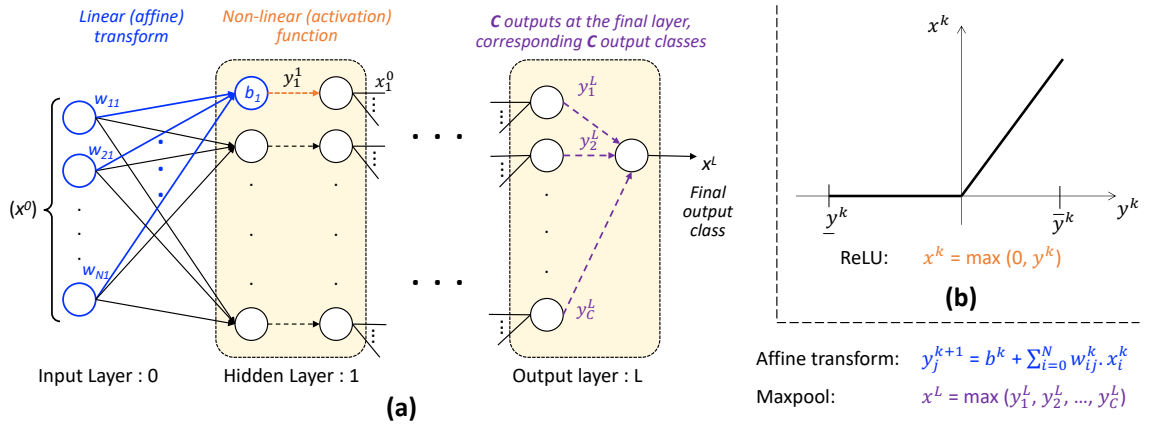


Fig. 1. (a) A Feed-forward fully-connected neural network, with L layers and C output classes, and (b) the ReLU activation function.

Each layer of the network F involves two transformations: a linear (affine) and a non-linear transformation. Given N neurons/nodes in the layer k of the network, the linear transformation can be given by:

$$y_j^k = b_j^k + \sum_{i=0}^N w_{ij}^k x_i^{k-1} \quad (1)$$

w_{ij}^k represents the weight connecting neuron i from layer $k - 1$ to neuron j in the layer k , while b_j^k represents the bias parameter value corresponding neuron j of the layer k .

The non-linear transformation maps output of the linear transformation via a non-linear activation function. For the purpose of this paper, all NN layers, except the output layer, use Rectified Linear Unit (ReLU) activation function. As shown in Fig. 1(b), the ReLU is a piecewise linear function mapping negative inputs to zero, while using identity

mapping the non-negative inputs:

$$x^k = \max(0, y^k) \quad (2)$$

The choice of NN output is often based on the output with the highest values. As such, maxpool function is used as an activation function for layer L of the network:

$$x^L = \max(y_1^L, y_2^L, \dots, y_C^L) \quad (3)$$

Consider the small feed-forward fully-connected NN shown in Fig. 2. The input, hidden and output layers comprise of 2, 3 and 2 neurons, respectively. The hidden layer uses ReLU activation function while the output layer makes use of maxpool function to provide the network's decision. The aforementioned network will be used as the running example in rest of the paper to visualize critical concepts.

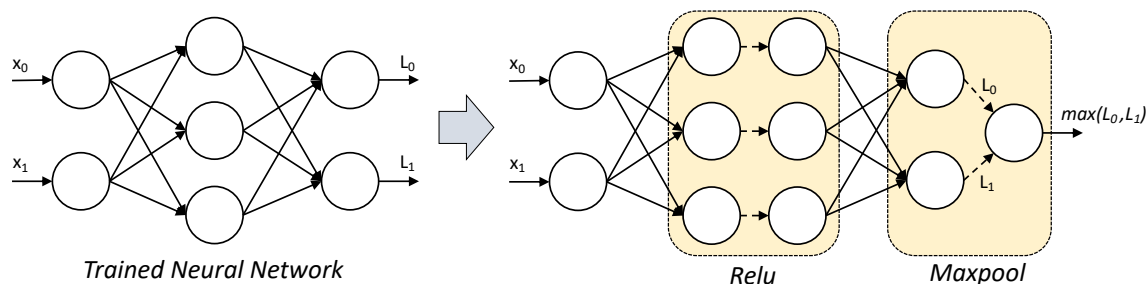


Fig. 2. A single hidden layer fully-connected NN using ReLU and maxpool activation functions.

3.2 Neural Network Properties

From the literature, it is known that the output classification of the NN may be incorrect under certain input conditions. The following provides formalism to some essential NN properties to ensure correct NN behavior under varying input conditions (like the incidence of noise).

Definition 3.2 (Robustness). Given a network $F : X \rightarrow Y$, F is said to be robust against the small noise Δx if the application of the noise to an arbitrary input $x \in X$ does not change the output classification of input by the network, i.e., $\forall \eta \leq \Delta x : F(x + \eta) = F(x)$.

Hence, by definition, a robust NN does not misclassify inputs in the presence of pre-determined noise Δx .

Definition 3.3 (Noise Tolerance). Given a network $F : X \rightarrow Y$, F is said to have a noise tolerance of Δx_{max} if the application of any noise up to Δx_{max} to an arbitrary input $x \in X$ does not change the output classification of input by the network, i.e., $\forall \eta \leq \Delta x_{max} : F(x + \eta) = F(x)$.

Robustness versus Noise Tolerance – A NN with a noise tolerance of Δx_{max} is robust against any noise Δx such that $\Delta x \leq \Delta x_{max}$. Hence, noise tolerance is a stronger property compared to robustness. In other words, noise tolerance provides (an estimate of) the upper bound of the noise that the network F can withstand, without showing any discrepancies in its normal behavior, i.e., without compromising the robustness of the network.

Definition 3.4 (Training/Robustness Bias). Let $x_1 \in X$ be an arbitrary input from the output class $A \subset Y$, while $x_2 \in X$ be an arbitrary input from the output class $B \subset Y$. Given a network $F : X \rightarrow Y$, F is said to be biased towards the class

A if the addition of noise Δx to x_1 does not cause any misclassification, but the addition of same noise to x_2 causes misclassification (i.e., $\exists \eta \leq \Delta x : (F(x_1 + \eta) = A) \wedge (F(x_2 + \eta) \neq B)$), for a significantly large number of noise patterns (η).

Robustness versus Training Bias – In simple terms, training bias is the robustness of the individual output classes of the trained network, to the same magnitude of noise. Such biased behavior in NNs can often be a result of the use of imbalanced datasets [3, 41], i.e., datasets with significant portion of the input samples belonging to a particular output class (class A), during NN training. Hence, the resulting network is robust to bounded noise applied only to the inputs from class A.

Definition 3.5 (Input Node Sensitivity). Given a network $F : X \rightarrow Y$, with the input domain comprising of N nodes $X = [X_1, X_2, \dots, X_N]$. Let $\Delta x = [\Delta x_1, \Delta x_2, \dots, \Delta x_N]$ be the noise applied to an arbitrary input $x \in X$, where the noise applied to each node is within the same bounds, i.e., $\Delta x_1 = \Delta x_2 = \dots = \Delta x_N$. The input node α is said to be insensitive if the application of noise to the node $\forall \eta_\alpha \leq \Delta x_\alpha : x_\alpha + \eta_\alpha$ does not change the output classification of the input x .

It must be noted that the sensitivity of an input node is analyzed independent of the remaining input nodes. This means, if the application of noise Δx_α to the node x_α does not change output classification of input x , the node is said to be insensitive regardless of what the noise (within the limits Δx) applied to the other input nodes may be.

Definition 3.6 (Safety). Given a network $F : X \rightarrow Y$, let $[\underline{X}, \overline{X}] \subseteq X$ be the valid input domain, and $[\underline{Y}, \overline{Y}] \subseteq Y$ be the safe output domain. The network F is said to be safe if all inputs within the valid domain maps to the safe output domain, i.e., $\forall x \in [\underline{X}, \overline{X}]. F(x) = y \text{ s.t. } y \in [\underline{Y}, \overline{Y}]$.

The safety property can also be subsumed by the concept of reachability, which requires any undesired output to be unreachable by all valid inputs. It must also be noted that while considering safety property, the maxpool activation in the output layer of NN is omitted to allow the analysis of a continuous output domain $[\underline{Y}, \overline{Y}]$, as opposed to discrete output classes.

3.3 Model Checking

Model checking is an automated formal verification approach, whereby specifications/desired properties are rigorously checked for a formal model/implementation given as a state–transition system, like a Kripke structure, as shown in Fig. 4(a).

Definition 3.7 (Kripke Structure). Let AP be the set of all possible atomic propositions for a given system. The Kripke structure M for the system is then a tuple $M = (S, I, \delta, L)$ such that:

- S is the set of all the possible states in the formal model M ,
- $I \subseteq S$ is the set of the possible initial states,
- $\delta \subseteq S \times S$ is the transition relation between the states, and
- $L : S \rightarrow 2^{AP}$ is the labeling function that defines the AP valid for each state in M .

In case the specification does not hold for the formal model, the model checker generally provides the counterexample in the form of a path to property violation. The path ρ in the model M is the sequence of states $\rho = S_i, S_{i+1}, \dots$ such that $\forall i. \delta(S_i, S_{i+1})$ holds. The paths may be *finite*, i.e., comprising of a fixed number of states, or *infinite*. The infinite paths result from self-loops or cycles in the model, and may contribute to the large number of states in the model, and hence,

leads to the infamous *state-space explosion* problem [4]. Additionally, the explicit declaration of state variables (as in explicit state model checking [31]) may also lead to the generation of a large number of states to encapsulate all possible behaviors in the formal model. This again leads to the state-space explosion.

Numerous abstraction approaches are available in the model checking literature to reduce the size of the formal model, hence avoiding state-space explosion and scaling the model checking for larger systems. Among the popular ones include: partial order reduction [4], counterexample guided abstraction refinement (CEGAR) [16], and bisimulation [45]. This paper leverages Bounded Model Checking (BMC) [7], Symbolic Model Checking (SMC) [44] and jump transitions [40] to optimize the formal models of NNs. BMC limits the length of paths by reducing number of reachable states, as explained later in the section. SMC provides a means to check system specifications without explicitly using a large number of states in the formal model by declaring the state variables symbolically, rather than explicitly. Jump transitions, on the other hand, compresses the states in the model for which the labeling function L provides the same valid set of AP , as depicted in Fig. 3.

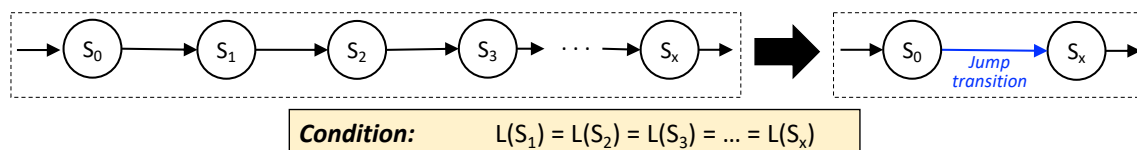


Fig. 3. Compressing Kripke structure using jump transition.

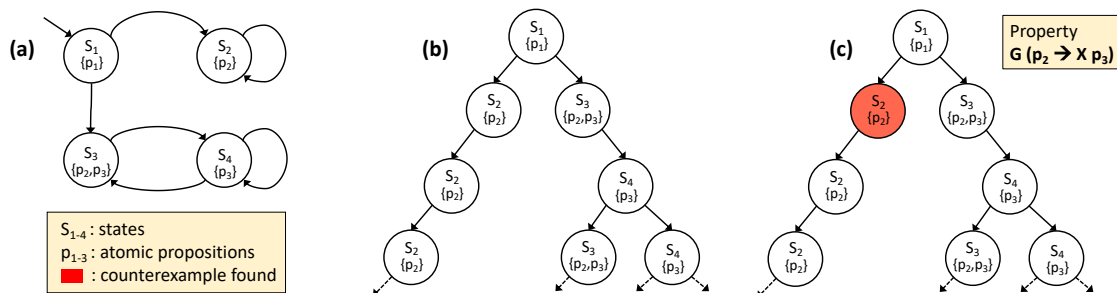


Fig. 4. (a) A simple finite state transition system with four states and three atomic propositions of interest; (b) Unwinding the transition system to generate the computation tree for bounded model checking; (c) searching the computation tree for the temporal property $G(p_2 \Rightarrow X p_3)$

Temporal logic is often the preferred formalism for defining the system properties in model checking. It allows the notion of time to be expressed in the propositions, using temporal operators like:

- *Next* (X): $X\phi$ holds true iff ϕ holds true in the next state.
- *Globally* (G): $G\phi$ holds true iff ϕ holds true in every state.
- *Eventually* (F): $F\phi$ holds true iff ϕ holds true in the current or (at least one of) the following states.

Given the formal model M and a property defined in temporal logic, model checking involves unwinding the model (see Fig. 4(b)) into a computation tree and transversing through the tree to search for a violation of the property (as shown in Fig. 4(c)). Given loops in the model, the unwinding of the model can potentially lead to paths of infinite

length, hence making model checking computationally infeasible. Hence, BMC is instead preferred, whereby the model is unwound a pre-defined number of times, so as to limit the maximum number of states on any given path in the tree by a bound k .

Verification versus Falsification – Falsification is an empirical approach to find evidence to disprove system properties [56]. Unlike verification, where the objective is to ensure an absence of erroneous behavior in the formal model, the objective of falsification is to merely find an evidence/counterexample presenting the erroneous behavior of the system’s model.

In terms of NNs, the falsification has been widely studied under the literature pertaining to adversarial inputs [1, 12, 38, 49]. NNs are already known to be vulnerable to noise [62], hence providing misclassification under the incidence of even minute magnitudes of noise. Falsification utilizes various optimization techniques to search region around the seed inputs (to the NNs) to identify this kind of misclassifying noise, i.e., the adversarial inputs. However, the techniques often lack the formal reasoning to conclude an absence of adversarial inputs in case one is not found. On the other hand, verification approaches rely on formal models and logical reasoning to ensure desired properties hold for the NNs. This makes them intrinsically different from the falsification techniques, albeit verification approaches like satisfiability solving and model checking also provide counterexample in case of property violation.

4 FORMAL ANALYSIS OF NEURAL NETWORKS (FANNET)

This section provides an overview of our base framework FANNet [48] that employs a model checking-based approach for the formal analysis of neural networks. The framework uses model checking to obtain the noise tolerance of the trained NNs. In addition, the counterexamples obtained from model checking are also leveraged to estimate sensitivity of the individual input nodes as well as detect any training bias in the trained NN.

4.1 Generating Kripke Structure of the Neural Networks

Consider the NN from our running example (also shown in Fig. 5). A binary noise, i.e., the noise with magnitudes either 0 or 1, is incident to the input nodes of the network. Recall that the model checking involves rigorous analysis of the state-transition system. So in case of explicit state model checking, there are four possible ways to apply noise to the input nodes. Hence, the resulting kripke structure contains four states leading from the initial state.

Additionally, the input can lead to either of the possible outputs, which provide the atomic propositions (AP) for the formal model. Hence, a transition from initial state, corresponding to any of the possible noise options, can lead to any possible outputs. This leads to the resulting formal model (i.e., the Kripke structure) to have $1 + nC$ states, where n is the number of noise options and C is the number of output classes in the network. Again, a rigorous analysis entails the possibility of network changing its state. Hence, the number of transitions making up the model adds to $nC(nC + 1)$. It must be noted that the hidden neurons are not presented in the formal model. This can be attributed to the use of jump transitions, which allows the compression of states having same set of AP .

4.2 Analyzing the Formal Network Model

Initially, the parameters and architectural details of the trained NN, as well as the bounds of the applied noise to network inputs, are used to define the formal model of the network (as described earlier). Defining parts of the model in the modular form (for instance, using neuron module in Fig. 6) allows concise high-level description of the model to be written in the model checker. The transitions between neurons (except the neurons in output layer) of the original

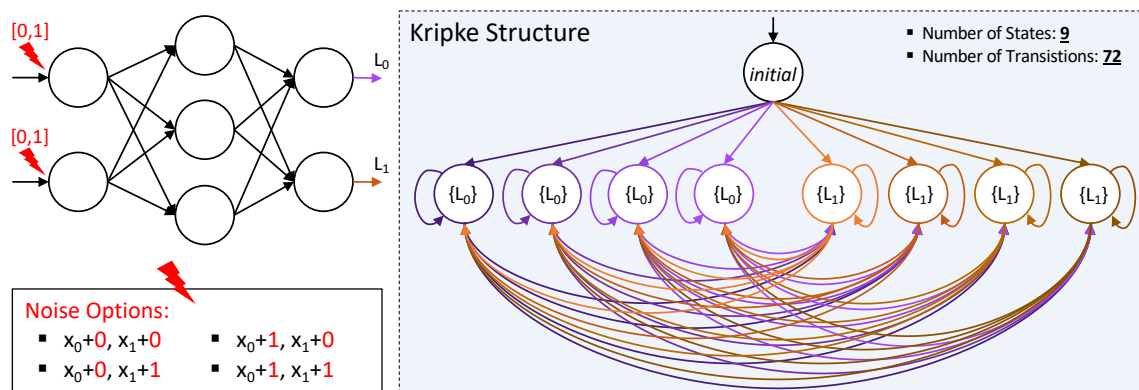


Fig. 5. The formal model (Kripke structure) for a small fully-connected NN (shown on top left), as generated by FANNet. A binary noise is incident to the network's inputs.

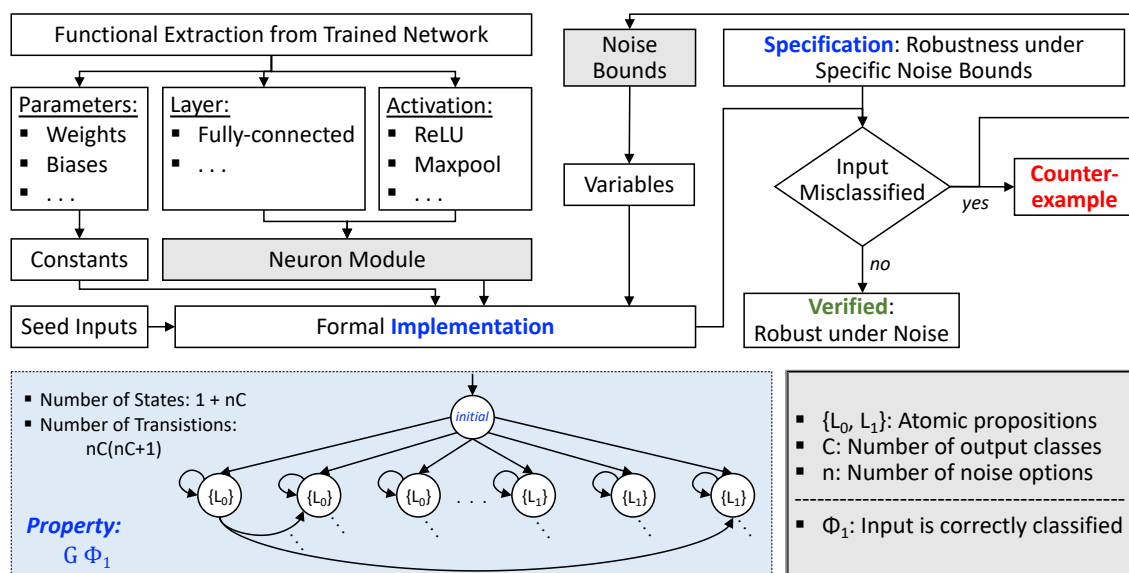


Fig. 6. The flowchart presenting the use of model checking for checking NN noise tolerance, as proposed in FANNet. The blue box indicates the Kripke structure generated by the model checker for NN with two ($= C$) output classes/atomic propositions.

NN are irrelevant to providing a change in output classification, i.e., for all paths leading up to the states representing neurons in output layers in the NN's model, the labeling provides same set of AP. Hence, these transitions can be compressed in the formal model using jump transitions, resulting in the model shown in Fig. 6.

The model checker then checks the robustness of the NN under the application of noise within the defined noise bounds. The framework considers the model with a single seed input at a time. Therefore, once the output is classified, the class remains unchanged. Hence, the use of bounded model checking entails completeness while checking the robustness of the NN model. The violation of the desired network specification is accompanied by a counterexample,

i.e., the specific noise vector that leads to misclassification of the seed input by the NN. Generally, large noise bounds are chosen initially. The model checking is then repeated while iteratively reducing the noise bounds, until network specifications hold valid. These noise bounds, Δx_{max} , represent the largest noise at which NN does not misclassify the input, and hence defines the noise tolerance of the network.

In addition to obtaining the noise tolerance, the framework can also be used to collect counterexamples, i.e., the noise vectors leading to misclassifications by the network. This is achieved by updating the formal specification with the negation of previously obtained counterexamples. Obtaining a significantly less number of misclassifying noise vectors that lead to a change in output class from A to other classes, than from other classes to class A , indicates a bias of the NN towards class A . A fine-grained analysis of the individual elements of the noise vectors, in turn, reflects on the predominant noise affecting/not affecting individual input nodes, hence unraveling the sensitivity of the nodes.

5 PROPOSED OPTIMIZATIONS FOR FORMAL NN ANALYSIS

FANNet was an initial model checking-based framework, relying on explicit state model checking for the analysis of NN properties. Given the efficient performance of explicit state model checking for software verification problems in literature [11, 17, 22], and the independence of our NN models on any particular hardware technology/components, the choice of the model checking approach used in FANNet was a logical first-step in the domain of model checking-based NN analysis.

However, as evident from the Kripke structure in Fig. 6, even a binary classifier will generate a formal model with $1 + 2n$ states, where n depends on the size and precision of the noise bounds used. For instance, consider a binary classifier trained on heart disease dataset (details of the experimental setup and further results for the aforementioned classifier are provided in Sections 6 and 7). Fig. 7 shows the average verification time taken for varying input noise. As the noise bounds/range increase, the size of the resulting Kripke structure also increases. This accounts for the large timing overhead for the verification.

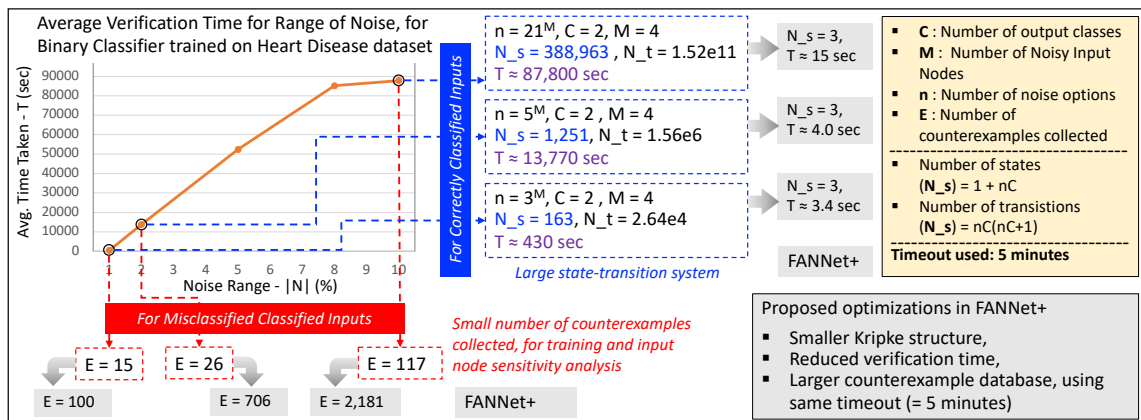


Fig. 7. Formal analysis of a binary classifier trained on heart disease dataset using FANNet. The framework delineates limited scalability due to: (a) large size of the network’s Kripke structure, (b) large verification time, and (c) small number of counterexamples collected within 5 minutes timeout. The proposed optimizations for FANNet+ improve scalability of NN analysis by addressing all the aforementioned limitations.

Moreover, for the precise analysis of NN’s training bias and input node sensitivity, a large number of counterexamples is required. This means, the model checking needs to be repeated multiple times, while iteratively updating the specification of this large formal model. Again, it can be observed from the case study in Fig. 7 that running FANNet for a small time duration like 5 minutes does not provide a large database of counterexamples for precise training bias and input node sensitivity analysis. These factors limit the scalability while increasing the timing overhead of FANNet.

This section elaborates on our proposed optimizations for reducing the size of the state–transition system (Kripke structure) leveraged by our enhanced framework, FANNet+. Moreover, two input splitting approaches are also proposed, which reduce the size of the input domain and hence improve the scalability and timing–efficiency of NN model. Hence, in addition to the multiple NN properties analyzed using FANNet, the proposed framework also allows the analysis of NN safety properties dealing with a large input domain, which was not viable earlier.

5.1 State-Space Reduction

As observed in the Kripke structure in Fig. 6, the state–space for the NN model contains multiple states leading to the same output class. This is because of the enumeration of the different noise combinations from the available noise bounds defining the formal model, leading to identical output states.

In contrast, FANNet+ proposes the use of SMC to reduce the identical output classes. The noise is added to the inputs symbolically, hence reducing the number of states in the model by a factor of approximately n . In terms of Kripke structure, the use of SMC to present noise symbolically is equivalent to merging of the states with the identical valid AP in the NN model. In other words, if the transition relations $\delta(S_a, S_b)$ and $\delta(S_a, S_c)$ hold, and the labelling function defines identical AP for the states S_b and S_c , i.e., $L(S_b) = L(S_c)$, then the states S_b and S_c can be merged.

CONJECTURE 5.1. *Given a model M with $S = [S_a, S_b, S_c]$ and $\delta = [(S_a, S_b), (S_b, S_b), (S_a, S_c), (S_c, S_c)]$ to be the set of all states and transition relations in the model, respectively, the states S_b and S_c can be merged iff $L(S_b) = L(S_c)$ holds.*

To understand the above state–space reduction, consider again the network from our running example. As shown in Fig. 8, the noise is added to the inputs symbolically, i.e., $(x_0 + noise)$ and $(x_1 + noise)$. Hence, all the states with the same AP (shown in Fig. 5) can be merged. The resulting model is considerably smaller, containing only $1 + C$ states and $C(C + 1)$ transitions, where C is the number of output classes.

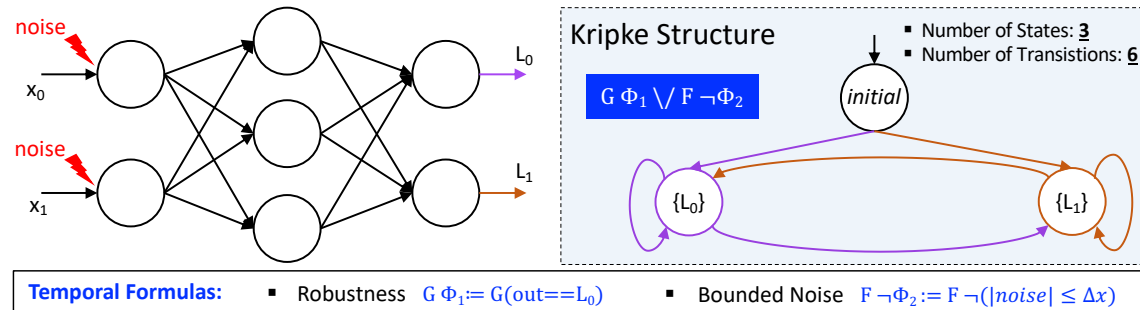


Fig. 8. The formal model for a small fully–connected NN (shown on left), as generated by FANNet+, with noise added symbolically to the inputs.

It must be noted that by using SMC to reduce the state–space of the model, the noise bounds are instead added to the existing formal specifications of the NN model. This is evident in the running example, where the bounds to the noise

are incorporated using $F \rightarrow \Phi_2$. This is added to the existing property $G\Phi_1$. Together, the temporal property states that either the output is *globally* correct or the noise *eventually* exceeds the noise bounds. Naturally, this incurs additional complexity for checking the specification (i.e., the stated robustness property), but for a considerably less number of states in the model. Overall, this has a positive impact on both the scalability and the timing efficiency of the approach (as will be shown by our experimental results in Section: 7).

Again from the Kripke structure in Fig. 6, it can be observed that the number of states with distinct valid *AP* depends on the number of output classes of the NN. However, model checking provides binary answers while checking the specifications, i.e., either the specification holds (UNSAT) or it is violated (SAT). This allows the number of states to be reduced even further by considering the output of the NN to be either “correctly classified” or “misclassified” instead being one of the C -output classes of the network. The same reduction is also applicable while checking other NN properties, like safety.

Overall, the model checking of the reduced state-space model is carried out as follows: NN parameters and architectural details are first used to define the NN formal model, as shown in the blue box in Fig. 9. A modular description of the model is again used for a concise high-level description of the model. The noise bounds and robustness property forms the specifications of the model. The model uses a fixed timeout to iteratively update the specification to collect counterexamples for the consequent analysis of NN properties, like training bias and input node sensitivity. The noise bounds are iteratively reduced until the noise tolerance of the trained network is obtained.

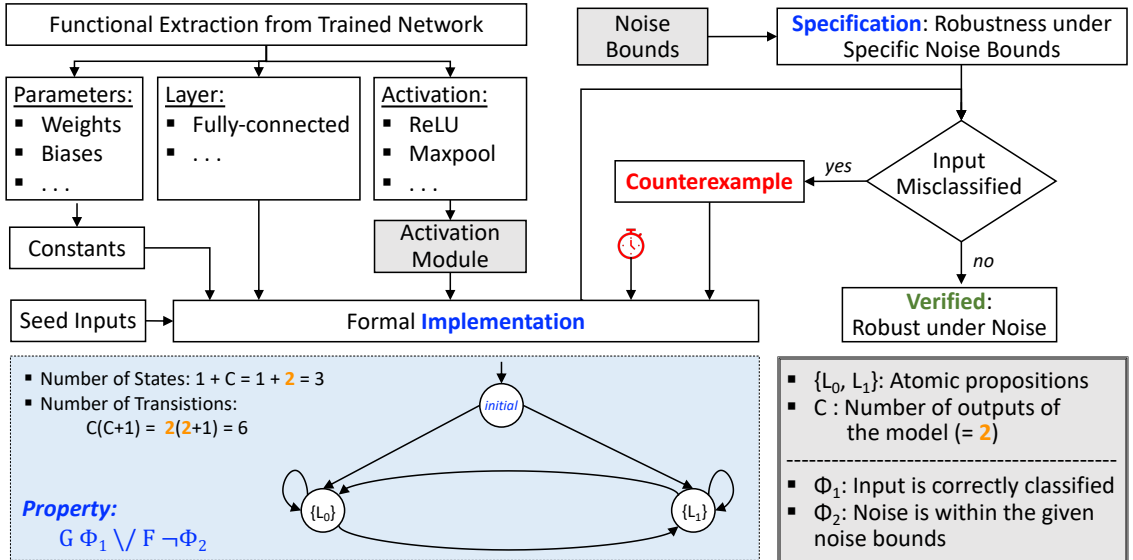


Fig. 9. The flowchart presenting the use of symbolic model checking for checking NN noise tolerance. The blue box indicates the optimized Kripke structure generated by the model checker for the NN.

5.2 Input Domain Segmentation

Noise tolerance analysis, as described above, makes use of seed inputs. Hence, model checker only verifies specification for one element of the input domain at a time. However, for NN properties like safety, the verification often needs to

be performed for the entire or subset of the input domain. This again requires a large Kripke structure, likely leading to state–space explosion. This paper proposes two approaches to resolve this problem: coarse–grain verification and random input segmentation.

5.2.1 Coarse–grain Verification. A rather straight–forward approach to verify a formal model with a large input domain is via sampling the input domain into discrete samples with regular intervals, i.e., with a constant sampling rate/step size. Depending on the size of the original NN, input domain and the available computational resources available to the model checker, the size of the input intervals can be fine–tuned. For NN specifications, for which the subset of input domain violating the specifications is large, the coarse–grain verification provides an efficient means to reduce the size of Kripke structure, while successfully finding any violations to the NN specifications. However, for input domains where property violation is a rare occurrence, the approach may overlook the property violations.

It must be noted that the use of SMC does not aid in the verification of systems with a large input domain, for highly non-linear systems like NNs. This is because, even though symbolic representation of input domain reduces the size of the generated Kripke structure, the addition of input bounds to the existing formal specification may make the specification too large to be verified by the model checker.

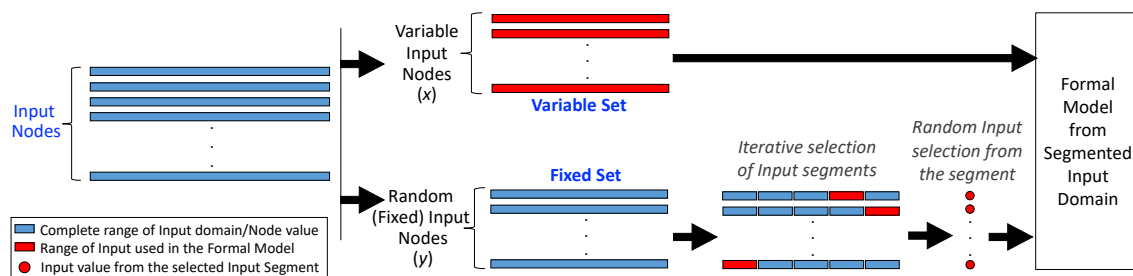


Fig. 10. Overview of Random Input Segmentation: the input nodes are split into *variable* and *fixed* sets, which are then fed to the formal NN model.

5.2.2 Random Input Segmentation. To address the challenge of dealing with a large input domain, this paper proposes the use of random input segmentation, as shown in Fig. 10. The overall idea here is to divide the input nodes into two mutually exclusive sets: the *variable* and the *fixed* input node sets. The model checking is then carried out using the inputs from the *variable* set represented symbolically while the discrete samples from the *fix* set represented as constants in the model. The details for the approach, also highlighted in Algorithm 1, are as follows:

- (1) Initially, for each input node, the upper and lower bounds of the (equally–spaced) input segments are calculated, as shown in Lines 3 – 4 of Algorithm 1. The number of input segments for each node (i.e., the bins per input node (X)) is pre–defined.
- (2) The input nodes for the *variable* set are then picked, while the remaining nodes form the *fixed* set. Line 9 of Algorithm 1 illustrates the selection of a single input node i for the *variable* set, while remaining nodes $Btemp$ form the *fixed* set. However, the algorithm can be modified to work for any number of nodes being assigned to either of the sets.

Algorithm 1 Random Input Segmentation

Input: Input Domain Bounds (I), Network Parameters (w, b, L, N),
Normalization Parameters (μ, ς), Bins per Input Node (X), Specification (Φ)
Output: Counterexample (CE)
Initialize: $CE \leftarrow []$

```
//Creating bins to split ranges of each input node
1: for  $i = 1:\text{Size}(I, 2)$  do ▷ For each input node
2:   for  $j = 1:X(i)$  do ▷ For each input segment
3:      $B[1][j][i] \leftarrow (\frac{I(2,i)-I(1,i)}{X(i)} \times (j-1)) + I(1, i)$ 
4:      $B[2][j][i] \leftarrow (\frac{I(2,i)-I(1,i)}{X(i)} \times j) + I(1, i)$ 
5:   end for
6: end for
//Segmentation
7: for  $i = 1:\text{Size}(I, 2)$  do
8:    $I' \leftarrow I$ 
9:    $Btemp \leftarrow B \setminus B\{:, :, i\}$ 
10:   $k \leftarrow \text{Size}(I, 2) - 1$  ▷ Total number of input nodes in fixed set
11:  for  $j_1 = 1:\text{Size}(Btemp\{:, :, 1\}, 2)$  do
12:    ...
13:    for  $j_k = 1:\text{Size}(Btemp\{:, :, k\}, 2)$  do
14:       $temp[1] \leftarrow \text{rand}(Btemp[1, j_1, 1], Btemp[2, j_1, 1])$ 
15:      ...
16:       $temp[k] \leftarrow \text{rand}(Btemp[1, j_k, k], Btemp[2, j_k, k])$ 
17:      for  $m = 1 : k$  do ▷ For updating  $I'$  with  $temp$  for input nodes from fixed set
18:        if  $i \leq m$  then
19:           $I'[m+1] \leftarrow temp[m]$ 
20:        else
21:           $I'[m] \leftarrow temp[m]$ 
22:        end if
23:      end for
24:       $temp \leftarrow [ ]$ 
25:       $CE \leftarrow \text{FANNET+}(I', w, b, L, N, \mu, \varsigma, \Phi)$  ▷ Model checking
26:      if  $CE \neq [ ]$  then return 1 ▷ Termination of code
27:    end if
28:  end for
29:  ...
30: end for
31: end for
```

- (3) Nested loops are used to pick the combination of segments for each input node in *fixed* set. For each combination of segments, a random discrete input value is picked for each input node, as shown in Lines 11 – 16 of Algorithm 1.
- (4) The input domain is then updated with constant random values for input nodes in the *fixed* set, as shown in Lines 17 – 23 of Algorithm 1.
- (5) The model checking is then performed with this updated input domain, shown by Line 25 of Algorithm 1.
- (6) If a counterexample corresponding to a property violation is obtained (as shown in Line 26 of Algorithm 1), i.e., the property is found to be SAT, model checking can be terminated. However, if no counterexample is found, the algorithm proceeds with the next discrete sample from the combination of segments of input nodes from the *fixed* set.
- (7) In turn, the process is repeated with a new splitting of input nodes into *variable* and *fixed* sets, as depicted in Lines 7 – 9 of Algorithm 1.

As the number of input nodes fed to the NN increase, the computation requirements (and subsequently the timing overhead) also increase. This “curse of dimensionality” is a known challenge with NN analysis in the literature [69]. However, by using random input segmentation, each splitting of the input nodes into the two sets and the following

model checking are completely independent. This provides an opportunity for high degree of parallelism to the approach by dealing with different combination of nodes from *fixed* and *variable* sets using a different core. This, in turn, reduces the timing-overhead of the analysis.

It must be noted that RIS is optimal for DNN verification (using FANNet+) iff $I^n > M^n \cdot \frac{I!}{M!M'!}$ hold, where n is the number of noise options, I is the total number of input nodes, M is the number of nodes in the variable set and M' the number of nodes in the fixed set ($I = M + M'$).

Soundness – As shown in Fig. 10 and Lines 17 – 23 of the Algorithm 1, the input domain I' contributing to the formal model analyzed by the model checker is the combination of the entire bounds of the input nodes from the *variable* set and random inputs from the selected segments of input nodes from the *fixed* set. Hence, this updated input domain is the proper subset of the original valid input domain I of the NN, i.e., $I' \subset I$. This preserves soundness of the framework.

Completeness – Since the updated input domain I' is the proper subset of domain I , the model checking using the domain entails incompleteness. This is the direct result of the Lines 14 – 16 of Algorithm 1, which bypass the exhaustive coverage of the segments of the input nodes from the *fixed* set. However, it must be noted that such incompleteness is essentially different from the incompleteness often observed in NN analysis literature [59, 60, 70, 71] arising from overapproximation of the input domain and/or activation functions, and hence leading to false positives in the analysis. The analysis based on our algorithm, in contrast, does not lead to any false positives.

5.3 FANNet+: An Integrated and Optimized Framework for Formal NN Analysis

The proposed optimizations reduce the size of NN’s Kripke structure as well as split the input domain into more manageable sub-domains. This improves the scalability and timing-efficiency of the framework, also allowing the analysis of NN properties beyond those addressed in FANNet. Fig. 11 summarizes our overall proposed framework FANNet+ for formal NN analysis.

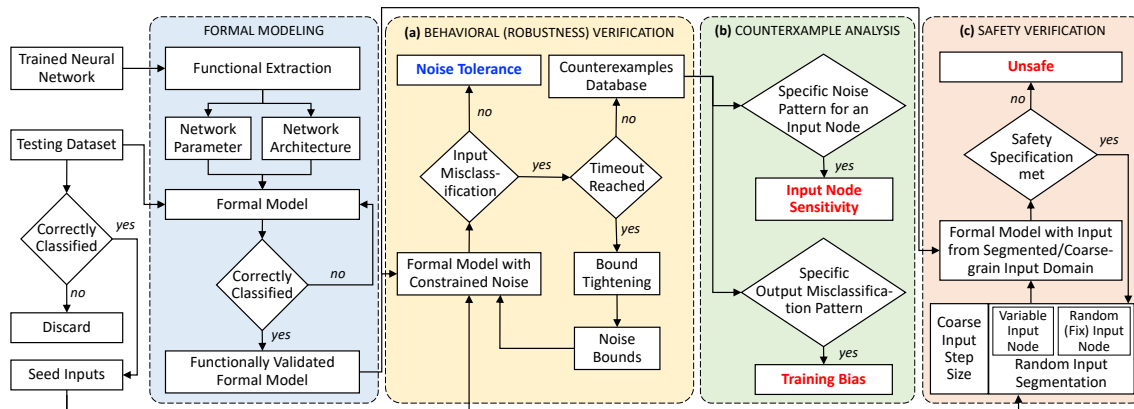


Fig. 11. FANNet+: the proposed (optimized) framework for the formal analysis of trained fully-connected neural networks. The framework is able to: (a) provide robustness verification and ultimately obtain noise tolerance of the network, (b) use the obtained counterexamples to analyze sensitivity of individual input nodes and check for the presence of training bias, and (c) provide safety verification using coarse-grain and/or randomly segmented input domain.

Initially, the formal model of the NN is defined in the appropriate syntax of the model checker, as indicated by the blue box in Fig. 11 and Algorithm 2. This requires the use of trained NN parameters and architectural details of the network. Input is often normalized prior to being sent to the NN (as shown in Line 2 of Algorithm 2). Some NNs may in turn also use inverse-normalization for the NN output (as shown in Line 14 of Algorithm 2). To validate the functional correctness of the model, the output of the model is checked for the known (testing) inputs.

Algorithm 2 Network Formalization and Property Checking

Input: Input (I), Network Parameters (w, b, L, N),
Normalization Parameters (μ, ζ), Specification (Φ)
Output: Counterexample (CE)
Initialize: $CE \leftarrow []$

```

1: function FANNET+( $I, w, b, L, N, \mu, \zeta, \Phi$ )
2:    $I_{norm} \leftarrow \frac{I - \mu}{\zeta}$  ▷ Input normalization
3:    $temp\_I \leftarrow I_{norm}$ 
4:   for  $i = 1 : L$  do
5:     for  $j = 1 : N(i)$  do
6:        $temp\_O[j] \leftarrow \sum(w[j][:][i]) \times temp\_I[j] + b[j][i]$  ▷ Fully-connected layer
7:       if  $temp\_O[j] < 0$  then
8:          $temp\_O[j] \leftarrow 0$  ▷ ReLU activation
9:       end if
10:    end for
11:     $temp\_I \leftarrow temp\_O$  ▷ Input propagation to next NN layer
12:  end for
13:   $Out_{norm} \leftarrow temp\_O$ 
14:   $Out \leftarrow (Out_{norm} \times \zeta) + \mu$  ▷ Output inverse-normalization
15:   $CE \leftarrow Property(\Phi, I, Out)$  ▷ Checking NN specification
16:  return  $CE$ 
17: end function

```

The robustness verification of the validated formal model is carried out using seed inputs from the testing dataset and noise bounds, as explained in Section 5.1. This is expressed in the yellow box in Fig. 11. Given the noise bounds $N\%$, the noise applied to seed inputs Δx is taken to be a percentage of original input node values, i.e., $\Delta x = x * (N/100)$. Hence, the robustness of the model is checked within L^∞ -ball (i.e., infinity norm) of radius Δx around the seed input. The NN specification is updated iteratively with the obtained counterexamples until a pre-defined timeout is reached. This allows the generation of a large counterexample database. In case the property holds before reaching the timeout, the model checking is immediately terminated. The noise bounds are iteratively reduced until the noise tolerance of the given network is obtained.

The counterexample database is then used in an empirical analysis to check the sensitivity of individual input nodes and detect any underlying training bias. This is shown by the green box in Fig. 11. The process is similar to the one used in FANNet. However, the improved timing-efficiency of our current framework allows model checking a large number of times within the pre-defined timeout. This provides a much larger counterexample database than was possible with FANNet, which in turn allows better analysis of the NN properties in question.

NN safety properties involve checking the NN model with a large input domain. The optimizations proposed in Section 5.2.2 allow safety verification of the validated formal model, as shown in the orange box in Fig. 11. Here, either coarse-grain verification or verification with random input segmentation can be opted. As mentioned earlier, the sampling rate (in coarse-grain verification) and the size of input segments (in random input segmentation) is chosen on the basis of the size of original NN, input domain and the available computational resources available to the model checker. The larger the network, input domain or computation resources available, the higher the sampling rate (or the smaller the input segment) needs to be.

6 EXPERIMENTS

This section describes the datasets and the NNs trained on them, which are used to demonstrate the application of FANNet+ for the analysis of NN properties.

6.1 Leukemia Type Identification

The leukemia dataset [28] is a collection of 72 samples of 7129 genetic attributes of leukemia patients. The dataset is split into 38 and 34 training and testing samples, respectively. Based on the genetic attributes, the dataset categorizes two types of leukemia: Acute Lymphoblast Leukemia (ALL), represented by approximately 70% of the training samples, and Acute Myeloid Leukemia (AML), represented by the remaining 30% of the training samples.

Minimum Redundancy and Maximum Relevance (mRMR) feature selection [39] was used to extract the 5 most important genetic attributes representing leukemia, which were then used for the training. A feed-forward fully-connected NN with single hidden layer and a total of 141 network parameters was trained for the dataset. The training and testing accuracies of the NN were 100% and 94%, respectively.

The following properties are analyzed for this NN: robustness (under constrained noise), noise tolerance, input node sensitivity, and training bias. The results of the analysis are presented in Section 7.

6.2 Heart Disease Prognosis

The heart disease dataset [19] provides the records for 13 attributes of the patients: among these, 4 attributes are represented by continuous values while remaining represent discrete attributes. The outputs indicate if the patients' blood vessels are narrowing, hinting to a heart disease. The dataset is split into training and testing datasets with 261 and 42 inputs, respectively. Approximately 55% of the samples from training dataset correspond to the case with narrowing blood vessels, while the remaining represent the samples with no significant narrowing of the blood vessels.

A feed-forward fully-connected NN with 3 hidden layers, and a total of 622 network parameters was trained for this dataset. The training and testing accuracies of the NNs were 90% and 86%, respectively.

To imitate real-world case scenarios, where the noise is much more likely to affect continuous variables as compared to discrete ones, noise was applied to the input nodes with continuous variables. This was in turn used for the analysis of robustness (under constrained noise), noise tolerance, input node sensitivity, and training bias. The results of the analysis are presented in Section 7.

6.3 Airborne Collision Avoidance System (ACAS Xu)

Airborne Collision Avoidance System (ACAS Xu) NNs belongs to the family of ACAS X systems that make use of the trajectories of ownship and intruder to ensure safety while maneuvering the ownship. The system consists of 45 NNs, which correspond to approximately different parts of the input domain. Each NN is feed-forward and fully-connected, with ReLU activation function, 6 hidden layers and 13,305 parameters.

Let i_1-i_5 be the NN inputs corresponding distance between ownship and intruder, and their heading angles and speeds, while o_1-o_5 be the ownship's maneuvering decisions namely clear-of-conflict, weak left/right and strong left/right. The NN's output decision corresponds to the output class with minimal value. Then the safety properties relevant to the NNs, which are also well-studied in the literature, include:

- (1) Given a large distance between ownship and intruder, with the intruder travelling at much slower speed than ownship, the clear-of-conflict remains below a certain threshold.

$$(i_1 \geq 55947.691) \wedge (i_4 \geq 1145) \wedge (i_5 \leq 60) \implies (o_1 \leq 1500) \quad (\text{P1})$$

- (2) Given a large distance between ownship and intruder, with the intruder travelling at much slower speed than ownship, the clear-of-conflict advisory does not have the highest value.

$$(i_1 \geq 55947.691) \wedge (i_4 \geq 1145) \wedge (i_5 \leq 60) \implies (o_2 > o_1) \vee (o_3 > o_1) \vee (o_4 > o_1) \vee (o_5 > o_1) \quad (\text{P2})$$

- (3) Given a constrained distance between ownship and intruder, with the intruder in line of ownship's translation and moving towards it, the NN's clear-of-conflict advisory is not minimal.

$$(1500 \leq i_1 \leq 1800) \wedge (-0.06 \leq i_2 \leq 0.06) \wedge (i_3 \geq 3.10) \wedge i_4 \geq 980 \wedge (i_5 \geq 960) \\ \implies (o_2 < o_1) \vee (o_3 < o_1) \vee (o_4 < o_1) \vee (o_5 < o_1) \quad (\text{P3})$$

- (4) Given a constrained distance between ownship and intruder, with the intruder in line of ownship's translation and moving away from it, but with a speed slower than that of the ownship, the NN's clear-of-conflict advisory is not minimal.

$$(1500 \leq i_1 \leq 1800) \wedge (-0.06 \leq i_2 \leq 0.06) \wedge (i_3 = 0) \wedge (i_4 \geq 1000) \wedge (700 \leq i_5 \leq 800) \\ \implies (o_2 < o_1) \vee (o_3 < o_1) \vee (o_4 < o_1) \vee (o_5 < o_1) \quad (\text{P4})$$

As indicated in Section 5, the analysis of safety properties involves a formal model with large input domains. Hence, coarse-grain verification and random input segmentation are used for the analysis of ACAS Xu NNs.

7 RESULTS AND ANALYSIS

We use NNs highlighted in the previous section to perform formal NN analysis on CentOS-7 systems running on Intel Core i9 – 9900X processors at 3.50GHz. The proposed framework FANNNet+ is implemented in Python, C++ and MATLAB, and uses NuXmv model checker [13] back end. The tools Reluplex [34] and Marabou [35] are implemented on virtualbox running Ubuntu 18.04, for comparison. The timeout used for NNs trained on leukemia and heart disease datasets is 5 minutes, while a timeout of 2 hours is used for ACAS Xu NNs.

This section first compares the timing and memory overhead of simulation-based testing (using MATLAB) with the FANNNet. The timing performance of FANNNet is then compared to FANNNet+, for robustness, noise tolerance, training bias and input node sensitivity analysis. Finally, the safety verification results for ACAS Xu NNs are presented, while comparing these results to those obtained from popular NN verification tools Reluplex and Marabou. It must be noted that the objective of comparison between FANNNet+ and SMT-based tools is to establish the consistency of results, not to compare timing-overhead since model checking is still fairly a new direction for DNN analysis.

7.1 Comparative Analysis of the Computational Overhead for Testing and FANNNet

Testing is generally considered more user friendly, as compared to model checking. However, the results for model checking are more rigorous, and hence provide more reliable behavioral guarantees than testing. We compared the performance of FANNNet with MATLAB-based testing. For testing, we define a matrix for all possible noise combinations, for a predefined noise bounds, before initializing the test. On the other hand, the model checker searches for noise combinations, non-deterministically, at run-time. Both experiments are based on the small NN trained on the Leukemia

dataset, as described in the previous section, since the timing and memory overhead of testing increases rapidly for large noise bounds for larger NNs. Both experiments run on the same seed inputs.

Considering the time taken until the termination of both experiments, the average timing requirement of the FANNet, although significantly higher than testing’s for the given experiment, increases at a slower rate than that for testing. This trend is illustrated in Fig. 12(a). On the other hand, the increase in average memory requirements of FANNet also increases at a significantly slower rate than testing, as shown in Fig. 12(b).

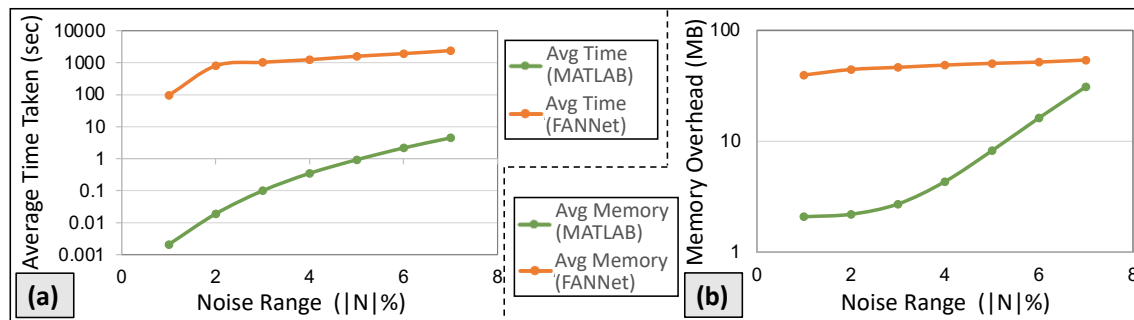


Fig. 12. (a) Timing, and (b) Memory overhead comparison, of analyzing the neural network trained on Leukemia dataset, between exhaustive testing (using MATLAB) and the model checking–based framework FANNet [48].

The trends for the average time and memory requirements of both experiments indicate that the strength of model checking is more prominent for larger NNs. As the size of the network grows, the Kripke structure system for NN grows, resulting in the increased latency and utilized memory resources. On the other hand, the computational requirements for (exhaustive) testing also increase with the increase in input noise range, often at a much higher rate than that for FANNet. This establishes the *advantage of formal NN analysis, even when the framework is not optimized.*

7.2 Behavioral (Robustness) Verification and Noise Tolerance Determination

As explained in Section 4, the Kripke structure model for NNs generated by FANNet is quite large, owing to the enumeration of noise applied to seed inputs. In contrast, the formal model generated by the FANNet+ is considerably smaller due to the optimizations for state–space reduction used. Hence, the framework provides same results (i.e., SAT or UNSAT) for both robustness verification and noise tolerance determination. However, the execution times of the frameworks are significantly different. Tables 1 and 2 summarise the the robustness of the seed inputs from the leukemia and heart disease datasets, respectively, under the incidence of increasing noise bounds.

FANNet versus FANNet+ – We run both frameworks for the NNs trained on the leukemia and the heart disease datasets. Figs. 13 shows the average execution time for verifying NNs for both datasets, for seed inputs robust to the applied noise. Identical noise bounds for seed inputs were used for both frameworks. Both frameworks use iterative noise reduction, leading to noise tolerance for NNs.

As observed in Fig. 14(a) and Fig.15 for NN trianed on leukemia dataset, both frameworks lead to the same noise tolerance i.e., 11% (also observe Table 1). The same is observed with NN trained on the heart disease dataset, having a noise tolerance of < 1%. However, the execution time for property verification is significantly larger for FANNet, as shown in Fig. 13. For the given NNs, FANNet+ provides a significant improvement over FANNet in terms of timing–cost,

Table 1. Robustness of seed inputs from leukemia dataset under varying noise bounds

Input	Result with Noise:				Input	Result with Noise:			
	11%	20%	30%	40%		11%	20%	30%	40%
1	UNSAT	UNSAT	UNSAT	UNSAT	17	UNSAT	UNSAT	UNSAT	UNSAT
2	UNSAT	UNSAT	UNSAT	UNSAT	18	UNSAT	UNSAT	UNSAT	UNSAT
3	UNSAT	UNSAT	UNSAT	UNSAT	19	UNSAT	UNSAT	UNSAT	UNSAT
4	UNSAT	UNSAT	UNSAT	UNSAT	20	UNSAT	SAT	SAT	SAT
5	UNSAT	UNSAT	UNSAT	UNSAT	21	UNSAT	UNSAT	UNSAT	UNSAT
6	UNSAT	UNSAT	UNSAT	UNSAT	22	UNSAT	UNSAT	UNSAT	UNSAT
7	UNSAT	UNSAT	UNSAT	UNSAT	23	UNSAT	UNSAT	UNSAT	UNSAT
8	UNSAT	UNSAT	UNSAT	UNSAT	24	UNSAT	UNSAT	UNSAT	SAT
9	UNSAT	UNSAT	UNSAT	UNSAT	25	UNSAT	UNSAT	SAT	SAT
10	UNSAT	UNSAT	UNSAT	UNSAT	26	UNSAT	UNSAT	UNSAT	UNSAT
11	UNSAT	UNSAT	UNSAT	UNSAT	27	UNSAT	SAT	SAT	SAT
12	UNSAT	UNSAT	UNSAT	UNSAT	28	UNSAT	UNSAT	UNSAT	UNSAT
13	UNSAT	UNSAT	UNSAT	UNSAT	29	UNSAT	UNSAT	SAT	SAT
14	UNSAT	UNSAT	UNSAT	UNSAT	30	UNSAT	SAT	SAT	SAT
15	UNSAT	UNSAT	UNSAT	SAT	31	UNSAT	UNSAT	UNSAT	UNSAT
16	UNSAT	UNSAT	UNSAT	UNSAT	32	UNSAT	UNSAT	UNSAT	SAT

Table 2. Robustness of seed inputs from heart disease dataset under varying noise bounds

Input	Result with Noise:				Input	Result with Noise:			
	2%	5%	8%	10%		2%	5%	8%	10%
1	UNSAT	UNSAT	UNSAT	UNSAT	19	UNSAT	SAT	SAT	SAT
2	UNSAT	UNSAT	UNSAT	UNSAT	20	UNSAT	UNSAT	UNSAT	UNSAT
3	UNSAT	UNSAT	UNSAT	UNSAT	21	UNSAT	UNSAT	UNSAT	UNSAT
4	UNSAT	UNSAT	SAT	SAT	22	SAT	SAT	SAT	SAT
5	UNSAT	UNSAT	UNSAT	UNSAT	23	SAT	SAT	SAT	SAT
6	UNSAT	UNSAT	UNSAT	UNSAT	24	UNSAT	UNSAT	UNSAT	UNSAT
7	UNSAT	UNSAT	UNSAT	UNSAT	25	UNSAT	UNSAT	UNSAT	UNSAT
8	UNSAT	UNSAT	UNSAT	UNSAT	26	UNSAT	UNSAT	UNSAT	UNSAT
9	UNSAT	SAT	SAT	SAT	27	SAT	SAT	SAT	SAT
10	UNSAT	SAT	SAT	SAT	28	UNSAT	UNSAT	UNSAT	UNSAT
11	UNSAT	UNSAT	UNSAT	UNSAT	29	UNSAT	UNSAT	UNSAT	SAT
12	UNSAT	UNSAT	UNSAT	UNSAT	30	UNSAT	UNSAT	UNSAT	UNSAT
13	UNSAT	UNSAT	UNSAT	SAT	31	UNSAT	UNSAT	UNSAT	UNSAT
14	UNSAT	UNSAT	UNSAT	UNSAT	32	UNSAT	UNSAT	UNSAT	UNSAT
15	SAT	SAT	SAT	SAT	33	UNSAT	UNSAT	UNSAT	UNSAT
16	UNSAT	UNSAT	UNSAT	UNSAT	34	UNSAT	UNSAT	UNSAT	UNSAT
17	UNSAT	UNSAT	SAT	SAT	35	SAT	SAT	SAT	SAT
18	UNSAT	UNSAT	UNSAT	SAT	36	UNSAT	UNSAT	UNSAT	UNSAT

by reducing the timing overhead by a factor of up to 8000 times. This makes FANNet+ suitable for the analysis of relatively larger NNs.

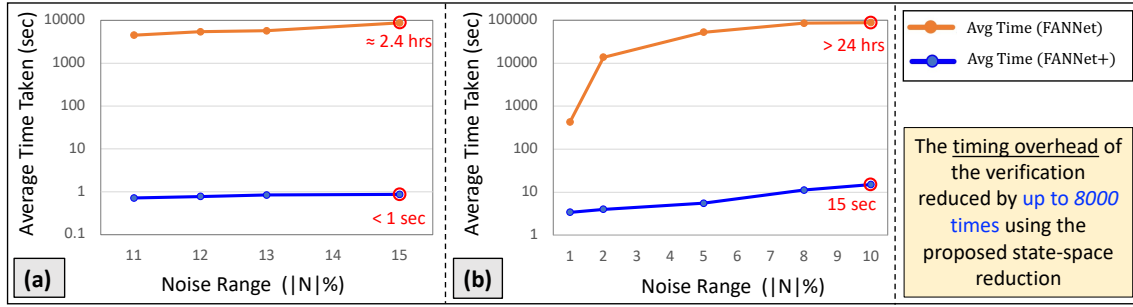


Fig. 13. Comparison of Timing Overhead using FANNet and FANNet+: (a) plots the results obtained from the NN trained on the leukemia dataset, while (b) plots results from the NN trained on the heart disease dataset.

7.3 Counterexample Analysis for detecting NN's Training Bias and Input Node Sensitivity

With the reduction in timing overhead, it is possible to run the framework for small timeout, and yet be able to collect a large database of misclassifying noise vectors, i.e., counterexamples. Analyzing the NN outputs for these counterexamples provide insights regarding training bias and input node sensitivity, as shown in Figs. 14 and 16.

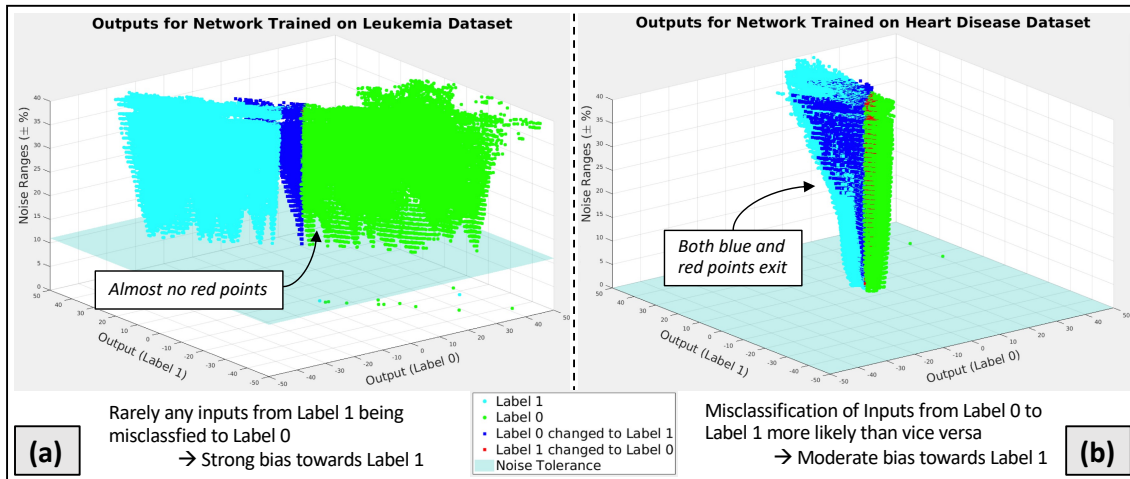


Fig. 14. Output classification of NNs trained on (a) Leukemia dataset and (b) Heart disease dataset, mapped with respect to the noise applied to seed inputs, using FANNet+. An unequal number of red and blue points indicates a bias in trained networks.

In Fig. 14(a), Label 1 corresponds to ALL leukemia while Label 0 corresponds to AML leukemia. On the other hand, Label 1 and 0 correspond to the cases with and without blood vessels narrowing, respectively, in Fig. 14(b). As observed in the figures, for the NN trained on leukemia dataset, even when the large noise is applied to inputs, ALL inputs are rarely misclassified to AML. From the description of available datasets (discussed in Section 6), it is known that training dataset for leukemia is significantly imbalanced, i.e., approximately 70% inputs belong to ALL. Hence, the obtained results indicate a strong bias in the resulting trained NN likely due to the imbalance in dataset.

On the contrary, for the NN trained on heart disease dataset, outputs from both classes are misclassified even though the misclassifications from Label 0 to Label 1 are more likely. The training dataset for heart disease does not have the

same class imbalance as the leukemia dataset. It contains inputs from the two input classes Labels 1 and 0 with a ratio of 55 : 45. This likely accounts for the relatively moderate bias observed in the NN.

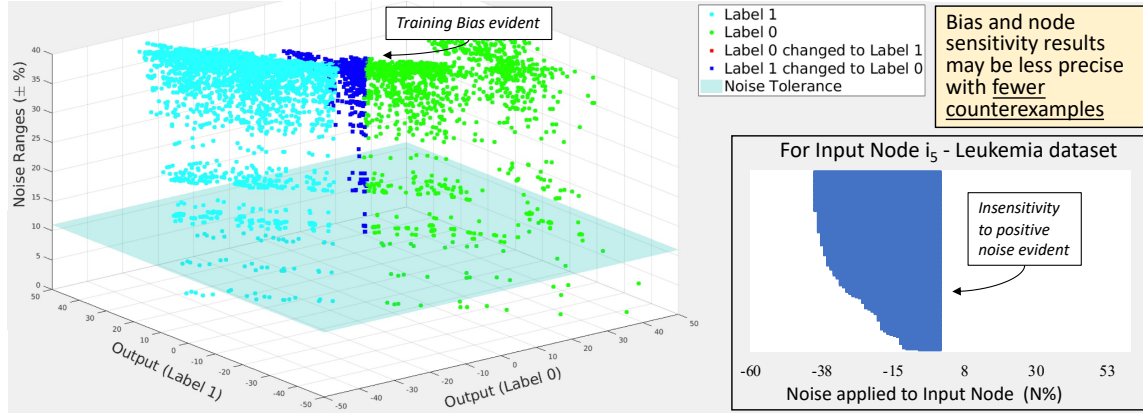


Fig. 15. Training bias and input node sensitivity of the NN trained on leukemia dataset, analyzed using the counterexample database obtained using FANNet.

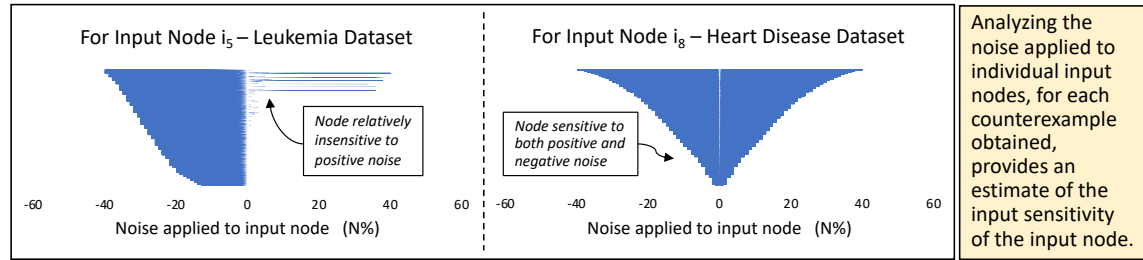


Fig. 16. Plots of noise applied to individual input nodes (using FANNet+), that lead to misclassification.

For the misclassifying noise vectors, observing noise applied to the individual input node provides insights to the sensitivity of the input nodes. For instance, input node i_5 from the NN trained on the leukemia dataset, shown in Fig. 16, was observed to delineate rarely any misclassifications for the positive values of the applied noise. This suggests the node to be insensitive to positive noise, for the trained NN. However, this was not the case for any of the input nodes for the NN trained on heart disease dataset. For instance, node i_8 in Fig. 16 gives an example of a typical input node that is not sensitive to any specific input noise.

FANNet versus FANNet+ – We performed the same experiment for NN trained on Leukemia using FANNet, as shown in Fig. 15. As discussed earlier, due to the large timing overhead of FANNet, the counterexamples obtained compose a smaller counterexample database. This is evident in the sparse 3D plot in Fig. 15. Hence, even though both FANNet and FANNet+ indicate the NN to be biased towards Label 1 and input node i_5 to be insensitive to noise, the results obtained by FANNet+ are more precise. For instance, given the noise bounds of 40%, Fig. 15 indicate node i_5 to be completely insensitive to any positive noise. However, FANNet+ (as shown in Fig. 16(a)) predicts the node to be relatively insensitive

to positive noise, but may still lead to NN misclassification with certain noise patterns. Hence, the larger counterexample database with FANNet+ is able to provide more precise results for training bias and input node sensitivity, as compared to FANNet.

7.4 Safety Verification

For NN properties, like safety, which involve large input domain, coarse-grain verification with input step sizes for ACAS Xu NNs as shown in Table 3, is first used. The verification for each property, for each NN, takes only a few seconds to complete. As mentioned earlier in Section 5, coarse-grain verification is suitable for NNs and properties where large segments of input domain violate the property. This does not hold true for ACAS Xu NNs. Hence, no counterexamples to property violation were found.

Table 3. Input step sizes used for coarse-grain verification of ACAS Xu safety properties.

Input Node	Step size for sampling input for each safety property			
	P1	P2	P3	P4
i_1	10,000	10,000	10^{-9}	1000
i_2	1	1	10^{-9}	10^{-1}
i_3	1	1	10^{-9}	–
i_4	500	500	10^{-9}	400
i_5	500	500	10^{-9}	400

Next, random input segmentation is deployed for the safety verification of ACAS Xu properties. The number of segments for each input node for the safety properties is given in Table 4. Based on the chosen *variable* and *fixed* sets, and the input segments of the nodes from *fixed* set, verification of each NN is split into multiple smaller verification sub-problems. As stated earlier, these verification problems are independent and hence, given sufficient computation resources, they can potentially all be verified in parallel. If any of these sub-problems return a SAT, the property is said to be violated for the NN. Likewise, if any of the sub-problems times out, the entire property is considered to have timed out, since the model checker is unable to find a result for a sub-section of the input domain. Otherwise, the verification is deemed to have terminated without a solution. It must be highlighted here that the framework does not return UNSAT since the use of *fixed* set introduces a certain degree of incompleteness, with respect to the input domain verified for the property. However, this notion of incompleteness is not the same as the *incompleteness of the formal model* observed in numerous state-of-the-art [59, 60, 70, 71], which may lead to false positive. On the other hand, FANNet+ does not lead to false positives in the results.

Table 4. Number of segments of input domain corresponding to every input node, for each property under analysis.

Input Node	P1	P2	P3	P4
i_1	3	3	2	2
i_2	4	4	3	3
i_3	4	4	2	1
i_4	2	2	4	4
i_5	2	2	4	4

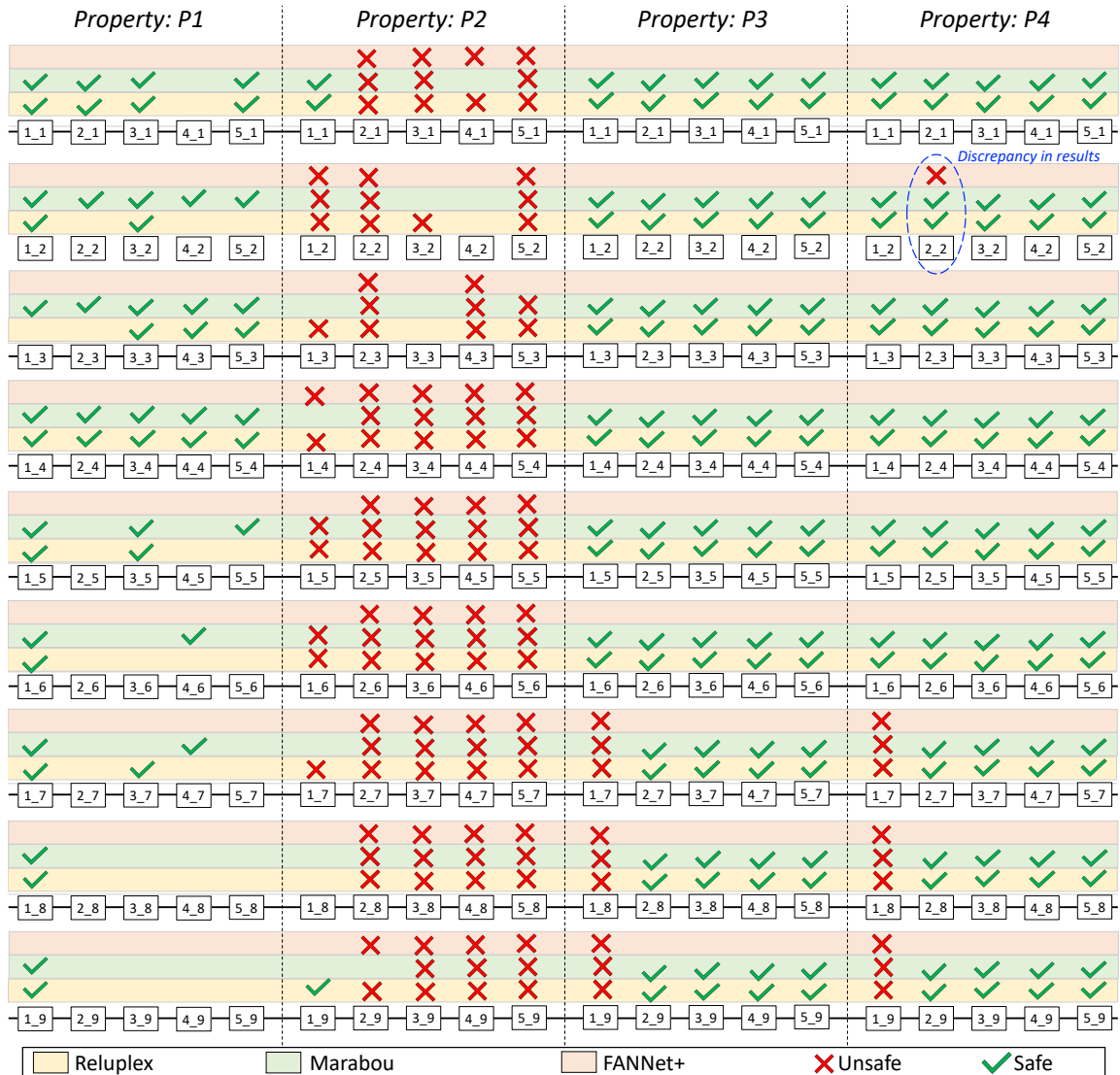


Fig. 17. Safety verification using Reluplex, Marabou and FANNet+: the frameworks either identify whether the bounded input domain is safe or unsafe for desired network safety properties, or remain inconclusive. In case of discrepancy in result, FANNet+ is found to provide correct result as opposed to the the other frameworks.

The results of the safety verification are compared to those obtained from Reluplex and Marabou. For all problems that provide SAT results with Reluplex and Marabou, FANNet+ is also able to find the property violation unless the verification times out. These are summarized in Fig. 17, where the success of FANNet+ in identifying unsafe networks is comparable to those of the state-of-the-art. It is interesting to note that FANNet+ was also able to find a property violation for the network 2_2 with property P4, although both Reluplex and Marabou return UNSAT for the stated

property. We confirmed the validity of the obtained counterexample using Maraboupy. The complete list of results for the safety properties using Reluplex, Marabou and FANNet+ is also provided in the appendix.

FANNet versus FANNet+ – As opposed to FANNet+, which leverages coarse-grain verification and random input segmentation to split input domain prior to verification, FANNet relies on bounds of entire input domain. Hence, the verification of safety properties of ACAS Xu NNs was infeasible with FANNet, even with a timeout of 24 hours.

8 CONCLUSION

Formally analyzing Neural Networks (NNs) is an actively sought research domain. Towards this end, a model checking-based framework FANNet was introduced earlier, which could verify robustness of trained NNs to constrained noise, and also analyze NNs' noise tolerance, input node sensitivity and any underlying training bias. This paper proposes a more scalable model checking-based framework FANNet+, which improves over FANNet in multiple directions. Firstly, it employs a state-space reduction strategy to ensure a more manageable size of the resulting state-transition system. Secondly, it introduced input domain segmentation approaches, including our novel random input segmentation approach, which uses a divide-and-conquer strategy to break the verification problem into smaller sub-problems. Thirdly, apart from the multiple NN properties mentioned earlier, the new framework FANNet+ extends the scope of NN analysis by adding the verification of safety properties to the framework. The aforementioned improvements were found to scale the framework for NN's with up to 80 times more NN parameters, while reducing the timing overhead by a factor of up to 8000 for the considered examples. The applicability of the framework was shown using multiple NNs, including the well-known ACAS Xu NNs benchmark.

ACKNOWLEDGMENTS

This work was partially supported by Doctoral College Resilient Embedded Systems which is run jointly by TU Wien's Faculty of Informatics and FH-Technikum Wien.

REFERENCES

- [1] Ahmed Aldahdooh, Wassim Hamidouche, Sid Ahmed Fezza, and Olivier Déforges. 2022. Adversarial example detection for DNN models: A review and experimental comparison. *Artificial Intelligence Review* (2022), 1–60.
- [2] Pranav Ashok, Vahid Hashemi, Jan Křetínský, and Stefanie Mohr. 2020. DeepAbstract: neural network abstraction for accelerating verification. In *Proc. ATVA*. Springer, 92–107.
- [3] Sikha Bagui and Kunqi Li. 2021. Resampling imbalanced data for network intrusion detection datasets. *Journal of Big Data* 8, 1 (2021), 1–41.
- [4] Christel Baier and Joost-Pieter Katoen. 2008. *Principles of model checking*. MIT press.
- [5] Pedro RAS Bassi and Romis Attux. 2021. A deep convolutional neural network for COVID-19 detection using chest X-rays. *Res. on Biomed. Engineering* (2021), 1–10.
- [6] Osbert Bastani, Yani Ioannou, Leonidas Lampropoulos, Dimitrios Vytiniotis, Aditya Nori, and Antonio Criminisi. 2016. Measuring neural net robustness with constraints. In *Proc. NeurIPS*. 2613–2621.
- [7] Armin Biere, Alessandro Cimatti, Edmund M Clarke, Ofer Strichman, and Yunshan Zhu. 2009. Bounded Model Checking. *Handbook of satisfiability* 185, 99 (2009), 457–481.
- [8] Elena Botoeva, Panagiotis Kouvaros, Jan Kronqvist, Alessio Lomuscio, and Ruth Misener. 2020. Efficient Verification of ReLU-based Neural Networks via Dependency Analysis. In *Proc. AAAI*. 3291–3299.
- [9] Rudy Bunel, Jingyue Lu, Ilker Turkaslan, P Kohli, P Torr, and P Mudigonda. 2020. Branch and bound for piecewise linear neural network verification. *JMLR* 21, 2020 (2020).
- [10] Rudy R Bunel, Ilker Turkaslan, Philip Torr, Pushmeet Kohli, and Pawan K Mudigonda. 2018. A unified view of piecewise linear neural network verification. In *Proc. NeurIPS*. 4790–4799.
- [11] Igor Buzhinsky, Antti Pakonen, and Valeriy Vyatkin. 2017. Explicit-state and symbolic model checking of nuclear I&C systems: A comparison. In *Proc. IECON*. IEEE, 5439–5446.

- [12] Nicholas Carlini and David Wagner. 2017. Towards evaluating the robustness of neural networks. In *Proc. S&P. IEEE*, 39–57.
- [13] Roberto Cavada, Alessandro Cimatti, Michele Dorigatti, Alberto Griggio, Alessandro Mariotti, Andrea Micheli, Sergio Mover, Marco Roveri, and Stefano Tonetta. 2014. The nuXmv Symbolic Model Checker. In *Proc. CAV*. 334–342.
- [14] Chih-Hong Cheng, Georg Nührenberg, Chung-Hao Huang, and Harald Ruess. 2018. Verification of Binarized Neural Networks via Inter-Neuron Factoring. In *Proc. VSTTE*. Springer, 279–290.
- [15] Chih-Hong Cheng, Georg Nührenberg, and Harald Ruess. 2017. Maximum resilience of artificial neural networks. In *Proc. ATVA*. Springer, 251–268.
- [16] Edmund Clarke, Orna Grumberg, Somesh Jha, Yuan Lu, and Helmut Veith. 2003. Counterexample-guided abstraction refinement for symbolic model checking. *JACM* 50, 5 (2003), 752–794.
- [17] Byron Cook, Daniel Kroening, and Natasha Sharygina. 2005. Symbolic model checking for asynchronous boolean programs. In *Proc. SPIN*. Springer, 75–90.
- [18] Martin Davis and Hilary Putnam. 1960. A computing procedure for quantification theory. *JACM* 7, 3 (1960), 201–215.
- [19] Dheeru Dua and Casey Graff. 2017. UCI Machine Learning Repository. <http://archive.ics.uci.edu/ml>
- [20] Souradeep Dutta, Susmit Jha, Sriram Sankaranarayanan, and Ashish Tiwari. 2018. Output range analysis for deep feedforward neural networks. In *Proc. NFM*. Springer, 121–138.
- [21] Ruediger Ehlers. 2017. Formal verification of piece-wise linear feed-forward neural networks. In *Proc. ATVA*. Springer, 269–286.
- [22] Cindy Eisner and Doron Peled. 2002. Comparing symbolic and explicit model checking of a software system. In *Proc. SPIN*. Springer, 230–239.
- [23] Yizhak Yisrael Elboher, Justin Gottschlich, and Guy Katz. 2020. An abstraction-based framework for neural network verification. In *Proc. CAV*. Springer, 43–65.
- [24] Andre Esteva, Alexandre Robicquet, Bharath Ramsundar, Volodymyr Kuleshov, Mark DePristo, Katherine Chou, Claire Cui, Greg Corrado, Sebastian Thrun, and Jeff Dean. 2019. A guide to deep learning in healthcare. *Nat. Medicine* 25, 1 (2019), 24.
- [25] Maximilian Fink, Ying Liu, Armin Engstle, and Stefan-Alexander Schneider. 2019. Deep Learning-Based Multi-scale Multi-object Detection and Classification for Autonomous Driving. In *Fahrerassistenzsysteme*. Springer, 233–242.
- [26] Timon Gehr, Matthew Mirman, Dana Drachler-Cohen, Petar Tsankov, Swarat Chaudhuri, and Martin Vechev. 2018. AI2: Safety and Robustness Certification of Neural Networks with Abstract Interpretation. In *Proc. SP. IEEE*, 3–18.
- [27] Gabriel Goh, Nick Cammarata, Chelsea Voss, Shan Carter, Michael Petrov, Ludwig Schubert, Alec Radford, and Chris Olah. 2021. Multimodal neurons in artificial neural networks. *Distill* 6, 3 (2021), e30.
- [28] Todd R Golub, Donna K Slonim, Pablo Tamayo, Christine Huard, Michelle Gaasenbeek, Jill P Mesirov, Hilary Coller, Mignon L Loh, James R Downing, Mark A Caligiuri, et al. 1999. Molecular classification of cancer: class discovery and class prediction by gene expression monitoring. *science* 286, 5439 (1999), 531–537.
- [29] Divya Gopinath, Guy Katz, Corina S Pasareanu, and Clark Barrett. 2017. DeepSafe: A data-driven approach for checking adversarial robustness in neural networks. *arXiv preprint arXiv:1710.00486* (2017), 1–17.
- [30] Geoffrey Hinton, Li Deng, Dong Yu, George Dahl, Abdel-rahman Mohamed, Navdeep Jaitly, Andrew Senior, Vincent Vanhoucke, Patrick Nguyen, Brian Kingsbury, et al. 2012. Deep neural networks for acoustic modeling in speech recognition. *Signal Process. magazine* 29, 6 (2012), 82–97.
- [31] Gerard J Holzmann. 2018. Explicit-state model checking. In *Handbook of Model Checking*. Springer, 153–171.
- [32] Xiaowei Huang, Marta Kwiatkowska, Sen Wang, and Min Wu. 2017. Safety verification of deep neural networks. In *Proc. CAV*. Springer, 3–29.
- [33] Itay Hubara, Matthieu Courbariaux, Daniel Soudry, Ran El-Yaniv, and Yoshua Bengio. 2016. Binarized Neural Networks. In *Proc. NeurIPS*, D. Lee, M. Sugiyama, U. Luxburg, I. Guyon, and R. Garnett (Eds.), Vol. 29. Curran Associates, Inc., 1–9.
- [34] Guy Katz, Clark Barrett, David L Dill, Kyle Julian, and Mykel J Kochenderfer. 2017. Reluplex: An efficient SMT solver for verifying deep neural networks. In *Proc. CAV*. Springer, 97–117.
- [35] Guy Katz, Derek A Huang, Duligur Ibeling, Kyle Julian, Christopher Lazarus, Rachel Lim, Parth Shah, Shantanu Thakoor, Haoze Wu, Aleksandar Zeljić, et al. 2019. The marabou framework for verification and analysis of deep neural networks. In *Proc. CAV*. Springer, 443–452.
- [36] Faiq Khalid, Hassan Ali, Muhammad Abdullah Hanif, Semeen Rehman, Rehan Ahmed, and Muhammad Shafique. 2020. FaDec: A Fast Decision-based Attack for Adversarial Machine Learning. In *Proc. IJCNN. IEEE*, 1–8.
- [37] Faiq Khalid, Muhammad Abdullah Hanif, Semeen Rehman, Rehan Ahmed, and Muhammad Shafique. 2019. TriSec: Training Data-Unaware Imperceptible Security Attacks on Deep Neural Networks. In *Proc. IOLTS. IEEE/ACM*, 188–193.
- [38] Faiq Khalid, Muhammad Abdullah Hanif, and Muhammad Shafique. 2021. Exploiting Vulnerabilities in Deep Neural Networks: Adversarial and Fault-Injection Attacks. *arXiv preprint arXiv:2105.03251* (2021).
- [39] Shujaat Khan et al. 2018. A novel fractional gradient-based learning algorithm for recurrent neural networks. *CSSP* 37, 2 (2018), 593–612.
- [40] Robt Kurshan, Vladimir Levin, and Hüsni Yenigün. 2002. Compressing transitions for model checking. In *Proc. CAV*. Springer, 569–582.
- [41] Guillaume Lemaître, Fernando Nogueira, and Christos K Aridas. 2017. Imbalanced-learn: A python toolbox to tackle the curse of imbalanced datasets in machine learning. *JMLR* 18, 1 (2017), 559–563.
- [42] Kang Liu, Benjamin Tan, Ramesh Karri, and Siddharth Garg. 2020. Training Data Poisoning in ML-CAD: Backdooring DL-based Lithographic Hotspot Detectors. *Proc. TCAD* 40, 6 (2020), 1244–1257.
- [43] Alessio Lomuscio and Lalit Maganti. 2017. An approach to reachability analysis for feed-forward ReLU neural networks. *arXiv preprint arXiv:1706.07351* (2017), 1–10.
- [44] Kenneth L McMillan. 1993. Symbolic model checking. In *Symbolic Model Checking*. Springer, 25–60.

- [45] R. Milner. 1982. *A Calculus of Communicating Systems*. Springer-Verlag, Berlin, Heidelberg.
- [46] Seyed-Mohsen Moosavi-Dezfooli, Alhussein Fawzi, Omar Fawzi, and Pascal Frossard. 2017. Universal adversarial perturbations. In *Proc. CVPR*. 1765–1773.
- [47] Nina Narodytska, Shiva Prasad Kasiviswanathan, Leonid Ryzhyk, Mooly Sagiv, and Toby Walsh. 2018. Verifying Properties of Binarized Deep Neural Networks. In *Proc. AAAI*. 6615–6624.
- [48] Mahum Naseer, Mishal Fatima Minhas, Faiq Khalid, Muhammad Abdullah Hanif, Osman Hasan, and Muhammad Shafique. 2020. FANNNet: Formal Analysis of noise tolerance, training bias and input sensitivity in Neural Networks. In *Proc. DATE*. IEEE, 666–669.
- [49] Nicolas Papernot, Fartash Faghri, Nicholas Carlini, Ian Goodfellow, Reuben Feinman, Alexey Kurakin, Cihang Xie, Yash Sharma, Tom Brown, Aurko Roy, et al. 2016. Technical report on the cleverhans v2. 1.0 adversarial examples library. *arXiv preprint arXiv:1610.00768* (2016).
- [50] Kexin Pei, Yinzhi Cao, Junfeng Yang, and Suman Jana. 2017. Deepxplore: Automated whitebox testing of deep learning systems. In *Proc. SOSP*. ACM, 1–18.
- [51] Luca Pulina and Armando Tacchella. 2010. An abstraction-refinement approach to verification of artificial neural networks. In *Proc. CAV*. Springer, 243–257.
- [52] Luca Pulina and Armando Tacchella. 2012. Challenging SMT solvers to verify neural networks. *AI Communications* 25, 2 (2012), 117–135.
- [53] Daniel Richardson. 1969. Some undecidable problems involving elementary functions of a real variable. *J. of Symbolic Log.* 33, 4 (1969), 514–520.
- [54] Karsten Scheibler, Leonore Winterer, Ralf Wimmer, and Bernd Becker. 2015. Towards Verification of Artificial Neural Networks. In *Proc. MBMV*. 30–40.
- [55] Andy Shih, Adnan Darwiche, and Arthur Choi. 2019. Verifying binarized neural networks by local automaton learning. In *Proc. AAAI Spring Symposium on VNN*. 1–8.
- [56] David Shriver, Sebastian Elbaum, and Matthew B Dwyer. 2021. Reducing dnn properties to enable falsification with adversarial attacks. In *Proc. ICSE*. IEEE, 275–287.
- [57] Md Amran Siddiqui, Jack W Stokes, Christian Seifert, Evan Argyle, Robert McCann, Joshua Neil, and Justin Carroll. 2019. Detecting Cyber Attacks Using Anomaly Detection with Explanations and Expert Feedback. In *Proc. ICASSP*. IEEE, 2872–2876.
- [58] João P Marques Silva and Karem A Sakallah. 2003. GRASP—a new search algorithm for satisfiability. In *The Best of ICCAD*. Springer, 73–89.
- [59] Gagandeep Singh, Timon Gehr, Matthew Mirman, Markus Püschel, and Martin Vechev. 2018. Fast and Effective Robustness Certification. In *Proc. NeurIPS*. 10802–10813.
- [60] Gagandeep Singh, Timon Gehr, Markus Püschel, and Martin Vechev. 2019. An Abstract Domain for Certifying Neural Networks. *PACMPL* 3, POPL (2019), 41.
- [61] Vivienne Sze, Yu-Hsin Chen, Tien-Ju Yang, and Joel S Emer. 2017. Efficient processing of deep neural networks: A tutorial and survey. *Proc. of the IEEE* 105, 12 (2017), 2295–2329.
- [62] Christian Szegedy, Wojciech Zaremba, Ilya Sutskever, Joan Bruna, Dumitru Erhan, Ian Goodfellow, and Rob Fergus. 2013. Intriguing properties of neural networks. *preprint arXiv:1312.6199* (2013), 1–10.
- [63] Vincent Tjeng, Kai Y Xiao, and Russ Tedrake. 2019. Evaluating robustness of neural networks with mixed integer programming. In *Proc. ICLR*. 1–21.
- [64] H. Tran, Stanley Bak, W. Xiang, and T. Johnson. 2020. Verification of Deep Convolutional Neural Networks Using ImageStars. In *Proc. CAV*. 18 – 42.
- [65] Hoang-Dung Tran, Xiaodong Yang, Diego Manzananas Lopez, Patrick Musau, Luan Viet Nguyen, Weiming Xiang, Stanley Bak, and Taylor T. Johnson. 2020. NNV: The Neural Network Verification Tool for Deep Neural Networks and Learning-Enabled Cyber-Physical Systems. In *Proc. CAV*. Springer, 3–17.
- [66] Shiqi Wang, Kexin Pei, Justin Whitehouse, Junfeng Yang, and Suman Jana. 2018. Efficient formal safety analysis of neural networks. In *Proc. NeurIPS*. 6367–6377.
- [67] Shiqi Wang, Kexin Pei, Justin Whitehouse, Junfeng Yang, and Suman Jana. 2018. Formal security analysis of neural networks using symbolic intervals. In *Proc. USENIX Security Symposium*. 1599–1614.
- [68] Wayne L Winston and Jeffrey B Goldberg. 2004. *Operations research: applications and algorithms*. Vol. 3. Thomson/Brooks/Cole Belmont, eCalif Calif.
- [69] Haoze Wu, Alex Ozdemir, Aleksandar Zeljić, Kyle Julian, Ahmed Irfan, Divya Gopinath, Sadjad Fouladi, Guy Katz, Corina Pasareanu, and Clark Barrett. 2020. Parallelization Techniques for Verifying Neural Networks. In *Proc. FMCAD*. 128–137.
- [70] W. Xiang, H. Tran, X. Yang, and T. T. Johnson. 2020. Reachable Set Estimation for Neural Network Control Systems: A Simulation-Guided Approach. *TNNLS* (2020), 1–10.
- [71] Weiming Xiang, Hoang-Dung Tran, and Taylor T Johnson. 2018. Output reachable set estimation and verification for multilayer neural networks. *TNNLS* 29, 11 (2018), 5777–5783.
- [72] Radosław R Zakrzewski. 2001. Verification of a trained neural network accuracy. In *Proc. IJCNN*, Vol. 3. IEEE, 1657–1662.
- [73] Erfan Zangeneh, Mohammad Rahmati, and Yalda Mohsenzadeh. 2020. Low resolution face recognition using a two-branch deep convolutional neural network architecture. *Expert Syst. with Applications* 139 (2020), 112854.

A SAFETY VERIFICATION RESULTS USING RELUPLEX, MARABOU AND FANNET+

This section provides the detailed results obtained after analyzing the safety properties P1-P4 for ACAS Xu networks using Reluplex [34], Marabou [35] and FANNet+. A consistent timeout of two-hours was used for all the experiments. As can be seen from the results in Tables A.1 and A.2, for all experiments, whenever the renowned tools Reluplex and/or Marabou find satisfying solution to the violation of property, FANNet+ is also able to find the counterexample(s) within the pre-defined timeout.

Table A.1. Results of verifying properties P1 and P2 for ACAS Xu Neural Networks

Network	Reluplex		Marabou		FANNet+	
	P1	P2	P1	P2	P1	P2
1_1	UNSAT	UNSAT	UNSAT	UNSAT	TO	TO
1_2	UNSAT	SAT	UNSAT	SAT	TO	SAT
1_3	TO	SAT	UNSAT	TO	TO	TO
1_4	UNSAT	SAT	UNSAT	TO	TO	SAT
1_5	UNSAT	SAT	UNSAT	SAT	TO	TO
1_6	UNSAT	SAT	UNSAT	SAT	TO	TO
1_7	UNSAT	SAT	UNSAT	TO	TO	TO
1_8	UNSAT	TO	UNSAT	TO	TO	TO
1_9	UNSAT	UNSAT	UNSAT	TO	TO	TO
2_1	UNSAT	SAT	UNSAT	SAT	TO	SAT
2_2	TO	SAT	UNSAT	SAT	TO	SAT
2_3	TO	SAT	UNSAT	SAT	TO	SAT
2_4	UNSAT	SAT	UNSAT	SAT	TO	SAT
2_5	TO	SAT	TO	SAT	TO	SAT
2_6	TO	SAT	TO	SAT	TO	SAT
2_7	TO	SAT	TO	SAT	TO	SAT
2_8	TO	SAT	TO	SAT	TO	SAT
2_9	TO	SAT	TO	TO	TO	SAT
3_1	UNSAT	SAT	UNSAT	SAT	TO	SAT
3_2	UNSAT	SAT	UNSAT	TO	TO	TO
3_3	UNSAT	TO	UNSAT	TO	TO	TO
3_4	UNSAT	SAT	UNSAT	SAT	TO	SAT
3_5	UNSAT	SAT	UNSAT	SAT	TO	SAT
3_6	TO	SAT	TO	SAT	TO	SAT
3_7	UNSAT	SAT	TO	SAT	TO	SAT
3_8	TO	SAT	TO	SAT	TO	SAT
3_9	TO	SAT	TO	SAT	TO	SAT
4_1	TO	SAT	TO	TO	TO	SAT
4_2	TO	TO	UNSAT	TO	TO	TO

Network	Reluplex		Marabou		FANNet+	
	P1	P2	P1	P2	P1	P2
4_3	UNSAT	SAT	UNSAT	SAT	TO	SAT
4_4	UNSAT	SAT	UNSAT	SAT	TO	SAT
4_5	TO	SAT	TO	SAT	TO	SAT
4_6	TO	SAT	UNSAT	SAT	TO	SAT
4_7	TO	SAT	UNSAT	SAT	TO	SAT
4_8	TO	SAT	TO	SAT	TO	SAT
4_9	TO	SAT	TO	SAT	TO	SAT
5_1	UNSAT	SAT	UNSAT	SAT	TO	SAT
5_2	TO	SAT	UNSAT	SAT	TO	SAT
5_3	UNSAT	SAT	UNSAT	SAT	TO	TO
5_4	UNSAT	SAT	UNSAT	SAT	TO	SAT
5_5	TO	SAT	UNSAT	SAT	TO	SAT
5_6	TO	SAT	TO	SAT	TO	SAT
5_7	TO	SAT	TO	SAT	TO	SAT
5_8	TO	SAT	TO	SAT	TO	SAT
5_9	TO	SAT	TO	SAT	TO	SAT

SAT: satisfiable solution found

TO: timeout (execution time exceeded 2 hours)

UNSAT: property unsatisfiable

NF: no counterexample found

Table A.2. Results of verifying properties P3 and P4 for ACAS Xu Neural Networks

Network	Reluplex		Marabou		FANNet+	
	P3	P4	P3	P4	P3	P4
1_1	UNSAT	UNSAT	UNSAT	UNSAT	TO	NF
1_2	UNSAT	UNSAT	UNSAT	UNSAT	TO	TO
1_3	UNSAT	UNSAT	UNSAT	UNSAT	TO	TO
1_4	UNSAT	UNSAT	UNSAT	UNSAT	TO	NF
1_5	UNSAT	UNSAT	UNSAT	UNSAT	TO	NF
1_6	UNSAT	UNSAT	UNSAT	UNSAT	TO	TO
1_7	SAT	SAT	SAT	SAT	SAT	SAT
1_8	SAT	SAT	SAT	SAT	SAT	SAT
1_9	SAT	SAT	SAT	SAT	SAT	SAT
2_1	UNSAT	UNSAT	UNSAT	UNSAT	TO	TO
2_2	UNSAT	UNSAT	UNSAT	UNSAT	TO	SAT
2_3	UNSAT	UNSAT	UNSAT	UNSAT	TO	NF
2_4	UNSAT	UNSAT	UNSAT	UNSAT	TO	NF
2_5	UNSAT	UNSAT	UNSAT	UNSAT	TO	TO

Network	Reluplex		Marabou		FANNet+	
	P3	P4	P3	P4	P3	P4
2_6	UNSAT	UNSAT	UNSAT	UNSAT	TO	TO
2_7	UNSAT	UNSAT	UNSAT	UNSAT	TO	TO
2_8	UNSAT	UNSAT	UNSAT	UNSAT	NF	TO
2_9	UNSAT	UNSAT	UNSAT	UNSAT	TO	NF
3_1	UNSAT	UNSAT	UNSAT	UNSAT	TO	NF
3_2	UNSAT	UNSAT	UNSAT	UNSAT	TO	NF
3_3	UNSAT	UNSAT	UNSAT	UNSAT	TO	NF
3_4	UNSAT	UNSAT	UNSAT	UNSAT	TO	NF
3_5	UNSAT	UNSAT	UNSAT	UNSAT	TO	TO
3_6	UNSAT	UNSAT	UNSAT	UNSAT	TO	NF
3_7	UNSAT	UNSAT	UNSAT	UNSAT	TO	NF
3_8	UNSAT	UNSAT	UNSAT	UNSAT	TO	NF
3_9	UNSAT	UNSAT	UNSAT	UNSAT	TO	NF
4_1	UNSAT	UNSAT	UNSAT	UNSAT	TO	NF
4_2	UNSAT	UNSAT	UNSAT	UNSAT	TO	NF
4_3	UNSAT	UNSAT	UNSAT	UNSAT	TO	NF
4_4	UNSAT	UNSAT	UNSAT	UNSAT	TO	NF
4_5	UNSAT	UNSAT	UNSAT	UNSAT	TO	NF
4_6	UNSAT	UNSAT	UNSAT	UNSAT	TO	NF
4_7	UNSAT	UNSAT	UNSAT	UNSAT	TO	NF
4_8	UNSAT	UNSAT	UNSAT	UNSAT	TO	TO
4_9	UNSAT	UNSAT	UNSAT	UNSAT	TO	NF
5_1	UNSAT	UNSAT	UNSAT	UNSAT	TO	NF
5_2	UNSAT	UNSAT	UNSAT	UNSAT	NF	NF
5_3	UNSAT	UNSAT	UNSAT	UNSAT	TO	NF
5_4	UNSAT	UNSAT	UNSAT	UNSAT	TO	NF
5_5	UNSAT	UNSAT	UNSAT	UNSAT	TO	NF
5_6	UNSAT	UNSAT	UNSAT	UNSAT	TO	NF
5_7	UNSAT	UNSAT	UNSAT	UNSAT	TO	NF
5_8	UNSAT	UNSAT	UNSAT	UNSAT	TO	NF
5_9	UNSAT	UNSAT	UNSAT	UNSAT	TO	NF

SAT: satisfiable solution found
TO: timeout (execution time exceeded 2 hours)

UNSAT: property unsatisfiable
NF: no counterexample found

Interestingly, FANNet+ is also able to find violation to property **P4** for the network 2_2, i.e., the experiment for which both Reluplex and Marabou return UNSAT. The satisfying input leading to violation of the property, as found by FANNet+ is as follows: [1600, 3, 0, 1100, 720]